

PNNL-39452

Inverter Based Resource Performance Monitoring and Analysis

Prepared by the NASPI Engineering Analysis Task Team

October 2026

DISCLAIMER

This report was prepared as an account of work sponsored by an agency of the United States Government. Neither the United States Government nor any agency thereof, nor Battelle Memorial Institute, nor any of their employees, makes **any warranty, express or implied, or assumes any legal liability or responsibility for the accuracy, completeness, or usefulness of any information, apparatus, product, or process disclosed, or represents that its use would not infringe privately owned rights**. Reference herein to any specific commercial product, process, or service by trade name, trademark, manufacturer, or otherwise does not necessarily constitute or imply its endorsement, recommendation, or favoring by the United States Government or any agency thereof, or Battelle Memorial Institute. The views and opinions of authors expressed herein do not necessarily state or reflect those of the United States Government or any agency thereof.

PACIFIC NORTHWEST NATIONAL LABORATORY
operated by
BATTELLE
for the
UNITED STATES DEPARTMENT OF ENERGY
under Contract DE-AC05-76RL01830

Printed in the United States of America

Available to DOE and DOE contractors from the
Office of Scientific and Technical Information,
P.O. Box 62, Oak Ridge, TN 37831-0062;
ph: (865) 576-8401
fax: (865) 576-5728
email: reports@adonis.osti.gov

Available to the public from the National Technical Information Service
5301 Shawnee Rd., Alexandria, VA 22312
ph: (800) 553-NTIS (6847)
email: orders@ntis.gov <https://www.ntis.gov/about>
Online ordering: http://www.ntis.gov

PNNL-39452

Inverter Based Resource Performance Monitoring and Analysis

October 2026

Prepared by the NASPI Engineering Analysis Task Team

Priya Mana	Pacific Northwest National Laboratory
Kaustav Chatterjee	Pacific Northwest National Laboratory
Hamed Mohsenian-Rad	University of California Riverside
Wilsun Xu	University of Alberta
Shuchismita Biswas	Pacific Northwest National Laboratory
Bikal Pudasaini	Dominion Energy
Chetan Mishra	Dominion Energy
Luigi Vanfretti	Rensselaer Polytechnic Institute
T.J. Purcell	Dominion Energy
Jim Follum	Pacific Northwest National Laboratory
Slava Maslennikov	ISO New England
Qiang (Frankie) Zhang	ISO New England
Patrick Gravois	ERCOT
Renzo Kennneth Machaca Yapuchura	COES – ISO Peru
Joseph Dubeau	Florida Power & Light Company
Matthew Rhodes	Salt River Project
Evangelos Farantatos	Electric Power Research Institute
Hossein Mohsenzadeh-Yazdi	University of California Riverside
Palberz Khaledian	University of California Riverside
Koji Yamashita	University of California Riverside
Dmitry Kosterev	Bonneville Power Administration

Prepared for the U.S. Department of Energy under Contract DE-AC05-76RL01830

Pacific Northwest National Laboratory
Richland, Washington 99354

Summary

Over the past few decades, the electric power system has been undergoing a paradigm shift, largely driven by the widespread integration of inverter-based resources (IBRs) such as solar photovoltaics (PVs), wind turbines, and battery energy storage systems (BESS). These power generating resources, interfaced to the grid through power electronic converters, differ fundamentally from conventional synchronous generators in both their physical characteristics and control mechanisms. As the penetration of these technologies continues to increase, their performance and interactions with the grid have become increasingly important to bulk power system (BPS) reliability and security. Accordingly, all grid-connected resources must operate in a manner that supports reliable system performance and complies with applicable reliability requirements and industry standards, necessitating adequate monitoring to verify compliance.

Given the critical role of monitoring in the reliable integration of IBRs, it is essential to understand existing capabilities, identify current gaps, and define future needs. Initiatives such as the Novel Applications for Synchronized Power Instrumentation (NASPI), co-led by the U.S. Department of Energy's Office of Electricity, Pacific Northwest National Laboratory (PNNL), and the Electric Power Research Institute (EPRI), are investigating how advanced monitoring technologies can support the implementation of evolving grid standards, including IEEE 2800, and enhance the stability and reliability of power systems with high IBR penetration.

The IBR Performance Response and Analytics Monitoring (IPRAM) task force under NASPI's Engineering Analysis Task Team (EATT) was established to bring together industry experts at various stages of IBR deployment who are applying monitoring solutions to maintain a stable and reliable grid. The task force, which includes experts from the electric power industry, research institutions, and academia, met at the annual NASPI Working Group meetings and virtually through IPRAM task force meetings to discuss existing measurement and analytics capabilities as well as advanced options for the future. This report was developed through the task force's discussions, written contributions, and participant questionnaires. It is intended to serve as a reference for the industry, offering fundamental information on monitoring methods appropriate for IBRs, documenting some of the collective experiences across utilities, and presenting discussions on several of the advanced methods currently available for IBR monitoring and analytics.

This report examines the motivation, considerations, and methods for monitoring IBRs and analyzing their performance in a grid that is increasingly changing due to the integration of power electronics-based generation and loads. The behaviors most relevant to IBR performance often occur on time scales and in forms that conventional supervisory control and data acquisition (SCADA) cannot capture. Thus, this report focuses on applications of synchrophasor measurements produced by phasor measurement units (PMUs) and synchro-waveform measurements from waveform measurement units (WMUs). PMUs estimate voltage and current phasors from sampled AC waveforms and report at typical rates of 30 or 60 frames per second, which is well suited to capturing system dynamics, low-frequency oscillations, and wide-area situational awareness. However, a key limitation is that PMUs assume sinusoidal waveforms and therefore cannot fully represent the non-sinusoidal behavior that can arise with IBRs. This limitation motivates the use of synchro-waveform measurements, also known as point-on-wave (POW) measurements. These measurements directly capture voltage and current waveforms at high sampling rates and preserve a much wider portion of the frequency spectrum. POW measurements are particularly well suited for detecting IBR behavior, which

can vary significantly within a short span of time, and for capturing detailed system behavior that may be essential for diagnosing IBR performance.

The report discusses several real-world use cases that demonstrate the value of high-resolution monitoring for IBRs. These include analysis of emerging dynamic behaviors, oscillation detection, oscillation source localization, monitoring, diagnostics, and fault response analysis. The real-world experiences reinforce that correct measurement placement and synchronized comparison are essential to interpreting IBR behavior correctly.

The report also discusses advanced analytics to further expand the capabilities of these measurements. These include the use of interharmonics to understand the oscillatory behavior of IBRs, advanced modeling and prediction of IBR dynamic responses, and the use of measurements to automatically evaluate the response of generators to system events.

The report concludes that PMU-based monitoring remains indispensable for wide-area situational awareness, and real-world deployments demonstrate their practical value for both detecting dynamic events and informing operational decisions. POW monitoring complements this by providing the detailed waveform information needed to address non-sinusoidal behavior and fast dynamics associated with IBRs. The report therefore advocates a hybrid monitoring approach of leveraging both PMU and POW technologies and aligning them with status, event, and supervisory context as the most effective path toward ensuring reliability, stability, and efficient operation as power systems continue to transition to higher penetrations of IBRs.

Acknowledgments

This work was supported by the U.S. Department of Energy (DOE) Office of Critical Minerals and Energy Innovation (CMEI) under the Integrated Energy Systems Office (IESO) Award Number 38411 and DOE's Office of Electricity (OE). The authors gratefully acknowledge the guidance and support of DOE sponsors Dexter Newton (CMEI\IESO) and Sandra Jenkins (OE). The views expressed herein do not necessarily represent the views of the U.S. DOE or the United States Government.

This report is the work of NASPI (Novel Applications for Synchronized Power Instrumentation), a DOE-OE initiative co led by Pacific Northwest National Laboratory (PNNL) and the Electric Power Research Institute (EPRI). The report was developed by the Inverter-Based Resource (IBR) Performance Response and Analytics Monitoring (IPRAM) task force under NASPI's Engineering Analysis Task Team (EATT). The task force would like to thank Jinho Kim from PNNL for providing technical review for this report and to Theresa Gilbride from PNNL for technical editing.

NASPI is a collaborative power-grid research network consisting of volunteer representatives from the utility industry, manufacturers, vendors, academia, national laboratories, and government agencies, that encourages high-speed, time-synchronized grid measurements and data sharing to facilitate reliable and secure operations of the power grid.

Acronyms and Abbreviations

AC	Alternating Current
AGMV	Automated Generator Model Validation
APPMV	Automatic Power Plant Model Validation
BESS	Battery Energy Storage System
BPA	Bonneville Power Administration
BPS	Bulk Power System
CAISO	California Independent System Operator
CDEF	Complex Dissipating Energy Flow
COES	Comité de Operación Económica del Sistema (ISO Peru)
COI	California-Oregon Intertie
COMTRADE	Common Format for Transient Data Exchange
CPOW	Continuous Point-on-Wave
CSV	Comma-Separated Values
DC	Direct Current
DDR	Dynamic Disturbance Recording / Recorder
DER	Distributed Energy Resource
DFT	Discrete Fourier Transform
DFR	Digital Fault Recorder
DOE	U.S. Department of Energy
DSO	Distribution System Operator
EATT	NASPI's Engineering Analysis Task Team
EMT	Electromagnetic Transient
ENTSO-E	European Network of Transmission System Operators for Electricity
ERCOT	Electric Reliability Council of Texas
ESAMS	EPRI Situational Awareness Monitoring System
FFR	Fast Frequency Response
FPL	Florida Power and Light
fps	Frames Per Second
FR	Fault Recording
FRM	Frequency Response Measurement
GO	Generator Owner
GPS	Global Positioning System
GSU	Generator Step-Up Transformer
Hz	Hertz
IBR	Inverter-Based Resource
IEEE	Institute of Electrical and Electronics Engineers

IEC	International Electrotechnical Commission
IPRAM	IBR Performance Response and Analytics Monitoring Task Force
ISO	Independent System Operator
ISO-NE	ISO New England
MVAR	Megavolt-Ampere Reactive
MW	Megawatt
NASPI	Novel Applications for Synchronized Power Instrumentation
NERC	North American Electric Reliability Corporation
NYISO	New York Independent System Operator
OG&E	Oklahoma Gas & Electric
OSL	Oscillation Source Location
P	Real Power
PCC	Point of Common Coupling
PDC	Phasor Data Concentrator
PES	Power & Energy Society (IEEE)
PFR	Primary Frequency Response
PGDA	Phasor Grid Dynamics Analyzer
PLL	Phase-Locked Loop
PMU	Phasor Measurement Unit
POC	Point of Connection
POI	Point of Interconnection
POM	Point of Measurement
POW	Point-on-Wave
PPM	Power Park Module
PQ	Power Quality
PRC	Protection and Control (NERC Standard Family)
PPC	Power Plant Controller
PSD	Power Spectral Density
PTP	Precision Time Protocol
PV	Photovoltaic
Q	Reactive Power
QSE	Qualified Scheduling Entity
RES	Reliability Entities
RfG	Requirements for Generators (EU Network Code)
RMS	Root Mean Square
RPA	Reference Point of Applicability
RTDMS	Real Time Dynamics Monitoring System
SCADA	Supervisory Control and Data Acquisition

SER	Sequence of Events Recording
SRP	Salt River Project
SSCIs	Sub-Synchronous Control Interactions
SSO	Sub-Synchronous Oscillation
SVC	Static Var Compensator
T&D	Transmission and Distribution
THD	Total Harmonic Distortion
TO	Transmission Owner
TSO	Transmission System Operator
UTC	Coordinated Universal Time
VRM	Voltage Response Measure
WECC	Western Electricity Coordinating Council
WMU	Waveform Measurement Unit
µPMU/micro-PMU	Micro-Phasor Measurement Unit

Contents

Summary ii
Acknowledgments iv
Acronyms and Abbreviations v
1.0 Introduction 12
2.0 Motivation 13
2.1.1 Unexpected Tripping During Disturbances 13
2.1.2 Low-Frequency Oscillations and Sub-Synchronous Control Interactions 14
2.1.3 High Frequency Harmonics 14
3.0 Monitoring Methods and Standards for an IBR-Rich Grid 16
3.1 Monitoring Locations 16
3.1.1 Types of Measurement Devices 17
3.1.2 Continuous vs. Triggered Data Acquisition 22
3.2 Standards for IBR Performance Monitoring 22
4.0 IBR Monitoring and Analysis Case Studies 25
4.1 Dominion Energy Case Study 25
4.1.1 Dynamic Performance Analysis of an Inverter-Based PV Plant During Sunrises and Sunset 25
4.1.2 Analyzing a Non-Sinusoidal Response from a Real-World Solar PV 27
4.2 ISO New England Case Study 28
4.2.1 Oscillation Detection, Characterization and Source Location 28
4.2.2 Power Plant Model Validation 30
4.3 ERCOT Case Study 30
4.4 Bonneville Power Administration Case Study 31
4.5 COES ISO-Peru Case Study 32
4.6 Florida Power and Light Case Study 35
4.7 IBR-Induced Oscillation Detected by PMU 35
4.7.1 Battery-Induced Oscillations, California, January 2022 35
4.7.2 Battery-Induced Oscillations, Arizona, 2023 36
4.7.3 Battery-Induced Oscillations, Cordova, Alaska 37
4.7.4 18-20 Hz IBR-Induced Oscillations, Kaua‘i Island, Hawaii, November 2021 37
4.8 Point-on-Wave Analysis of Unexpected IBR Responses to Transient Disturbances 38
5.0 IBR Performance Monitoring and Analytics - Proposed Advanced Methods 41
5.1 Interharmonics-Based IBR Oscillation Monitoring 41
5.1.1 Interharmonics Causing Phasor Oscillation 41

5.1.2 Field Examples of Oscillation Source Location 44
5.2 Modeling and Prediction of IBR Dynamic Response 46
5.3 Generator Scorecard 48
5.3.1 Frequency Response Measure (FRM) 48
5.3.2 Voltage Response Measure (VRM) 51
6.0 Conclusion 54
7.0 References 55

Figures

Figure 1. Schematic describing POM, POI, POC, and RPA. Adapted from (IEEE Std. 2800-2022, 2022). 16
Figure 2. MicroPMU measurements at a 4.3-MW solar farm in Riverside, CA: (a) solar production monitored over a period of 10 minutes; (b) magnified view of an abnormal inverter operation at 9:17 minutes. Source: (Mohsenian-Rad & Khaledian, 2022). 18
Figure 3. A microPMU monitor (μPMU_{PV}) is installed to track power fluctuations at the point of common coupling (PCC) of a 4.3-MW behind-the-meter solar farm in Riverside, CA. A second microPMU (μPMU_{Other}) is installed at the other side of the substation on another feeder as a reference. Source: (Mohsenian-Rad & Khaledian, 2022). 19
Figure 4. Inverter model calibration using measurement playback (Luo, 2023). 22
Figure 5. Simplified architecture of Synchrophasor Analysis Environment used by Dominion Energy to monitor its transmission network, March 2025. 25
Figure 6. Power spectral density analysis of the current magnitude signal at the output of a 105-MW photovoltaic plant during the perceived oscillation, revealing multiple peaks. 26
Figure 7. Spectrogram of the current magnitude signal at the output of the solar plant at a lower frequency range for five consecutive days. 26
Figure 8. Analysis of an atypical, poorly damped slow (<0.05 Hz) response from a transmission-level PV solar power plant triggered by a local line outage in Dominion Energy's power system showing unique square wave response is not due to inverter dynamics but is due to large feedback delays in the PPC: Left - Square VAR Oscillations from PV; right - Feedback Delay Estimation using V-Q Causality. 27
Figure 9. EMS Alarm Message Sample at ISO New England 28
Figure 10. OSL Alarm Email Message Sample for the January 11, 2019, EI oscillatory event. 28
Figure 11. NE-NY tie-line flow for a 0.15 Hz oscillation originating in Maine. 29
Figure 12. Dissipating energy flow plot on New England one-line diagram 29
Figure 13. Analytical results from SCADA data. 30
Figure 14. Control oscillation of an IBR plant at high power output 31

Figure 15. Disturbance-based model validation of an IBR plant. 32
Figure 16. Solar potential and IBR concentration are predominantly located in southern Peru. 33
Figure 17. Wind potential in Peru is predominantly along the coast and the mountain ridges. 33
Figure 18. Lower frequency (0.25 Hz) oscillations introduced by telecommunication failures in a BESS plant in Southern California, January 2022 (Agrawal, Bohlen, Hiebert, & Penne, 2024). 36
Figure 19. MicroPMU measurements detect oscillations in an island power system in Cordova, Alaska, due to a battery energy storage system (BESS) (Becejac, Follum, Vartanian, & Cain, 2020). 37
Figure 20. The locations of 68 IBRs with WMUs in Ontario, Canada, whose waveform responses to a system-wide disturbance caused by a 500-kV fault was studied in (Yazdi, Li, & Mohsenian-Rad, 2025). 38
Figure 21. Examples of the current waveforms for the IBR responses in each of 7 classes identified by applying pattern recognition on synchro waveform measurements. Source: (Yazdi, Li, & Mohsenian-Rad, 2025). 39
Figure 22. Sample time-domain waveform (a) and frequency-domain spectrum (b) of phase A current of a windfarm. 41
Figure 23. Mechanism of an interharmonic causing phasor oscillation. 42
Figure 24. Scheme for oscillation monitoring and source location. 44
Figure 25. A case of windfarm oscillations. 44
Figure 26. Sample time-domain waveform (a) and frequency-domain spectrum (b) of phase A current of WF3. 45
Figure 27. 63.5 Hz interharmonic power out of windfarms WF2 and WF3. 45
Figure 28. Three-phase voltage and current waveforms of a solar farm. 46
Figure 29. Spectrums of current and interharmonic power of the solar farm. 46
Figure 30. The process to model the dynamic response of IBRs to sub-cycle disturbances using waveform measurements: (a) a sub-cycle voltage oscillation event in the power system, which in turn causes agitation in the injected current by the IBR; (b) the corresponding differential waveforms that capture the signatures of the sub-cycle disturbance and the signatures of the sub-cycle response of the IBR; (c) a data-driven model for the input-output relationship between the sub-cycle disturbance and the sub-cycle response of the IBR. 47
Figure 31. Illustration of the inputs to the FRM calculation for Signature 2463 under Provider 10 in the Grid Event Signature Library (ORNL, LLNL, PNNL, 2024). 49
Figure 32. Summary of responses from two power plants for all frequency excursions analyzed during the field demonstration. Plant 1 shows inconsistent performance, while Plant 2 regularly adjusts active power up for under-frequency excursions and down for over-frequency excursions. 50
Figure 33. Simulation of a wind power plant's appropriate response in reactive power (bottom) to a sudden change in voltage at the point of interconnection (top). 52

Figure 34. Summary of all voltage excursions analyzed during the field demonstration. Clustering in quadrants 1 and 3 indicate that plants across the territory appropriately adjusted reactive power. 53

Tables

Table 1. Root cause investigation results for several IBR-induced oscillations observed in the Salt River Project (SRP) territory and their Western Electricity Coordinating Council (WECC) impact (Rhodes & and Goodrich, 2024). 37

1.0 Introduction

Inverter-based resources (IBRs) connect to the grid through power electronic interfaces. As a result, their electrical behavior and response to system disturbances are largely governed by converter and plant controls rather than the physical characteristics of synchronous machines. This evolution has increased the need for effective monitoring and analytics to evaluate IBR performance and support reliable grid operation.

Monitoring is essential for identifying IBR performance issues, verifying operational behavior, and supporting the implementation of evolving grid requirements, including IEEE 2800 (IEEE Std. 2800-2022, 2022). In response to these needs, the Novel Applications for Synchronized Power Instrumentation (NASPI) working group has supported efforts to assess and advance monitoring applications for power systems with increasing IBR penetration. A clear understanding of available monitoring technologies, existing limitations, and future analytical needs is necessary to support these efforts.

The IBR Performance Response and Analytics Monitoring (IPRAM) task force was established within NASPI's Engineering Analysis Task Team (EATT) to facilitate collaboration among industry, research, and academic experts involved in the deployment and assessment of IBRs. During the 2025 and 2026 NASPI Working Group meetings and additional IPRAM task force meetings, participants examined current measurement and analytics practices and discussed potential approaches for future monitoring applications. This report summarizes the task force's discussions, written contributions, and questionnaire responses. It is intended to provide an industry reference on monitoring methods applicable to IBRs, capture collective experience across utilities and other organizations, and describe selected advanced techniques for IBR monitoring and performance analytics.

The remainder of this report is organized as follows. Section 2.0 describes the differences between IBR and conventional generation resources and discusses the drivers for IBR monitoring. Section 3.0 describes current and new methods for monitoring in IBR-rich grids, including both synchrophasor-based methods and high-resolution point-on-wave (POW)-based measurement techniques. It also highlights relevant standards shaping current and future monitoring requirements. Section 4.0 presents real-world case studies showcasing practical applications, lessons learned, and ongoing initiatives. Section 5.0 discusses selected advanced methods and proposed analytics that represent the forefront of research and development in this area. Section 6.0 concludes the paper with key insights, challenges, and recommendations for future work.

2.0 Motivation

The behavior of IBRs during both normal operation and contingency scenarios can deviate significantly from the assumptions underlying traditional grid models developed around synchronous generation. Traditional power plants have synchronous spinning rotors that naturally slow down due to mechanical inertia when grid frequency drops due to a power interruption. IBRs like solar panels and battery energy storage systems have no moving parts; they rely entirely on high-speed power electronic converters and software control loops to interact with and to stabilize the grid. The converter decouples the resource's mechanical or electrochemical energy source from the grid and uses control algorithms to determine how the resource responds to voltage, frequency, and disturbances. The response of an IBR therefore depends on the converter controls, measurement systems, protection functions, operating limits, and interactions with other power electronic devices and the grid.

IBRs can respond much more rapidly than synchronous machines and can provide functions such as fast active-power modulation, reactive-power control, voltage support, and synthetic inertial response. Different control architectures can also have a significant impact of IBR response and performance. For example, a grid-following inverter uses measurements of grid voltage and frequency to synchronize their output, whereas grid-forming inverters are designed to establish or regulate a voltage waveform and act as a voltage-source. This flexibility allows inverter controls to be tailored to specific grid-support functions, but it also means that two resources with similar ratings may exhibit very different responses to the same disturbance. This paradigm shift introduces a new set of challenges in system stability and makes accurate models, appropriate control coordination, and high-quality monitoring essential for evaluating IBR performance.

While IBRs offer significant new capabilities and opportunities for the power system, their large-scale integration remains relatively recent. It is therefore essential to ensure that IBRs are integrated in a manner that supports reliable system operation and that their capabilities and performance are well characterized, monitored, and assessed in practice.

Through the early stages of IBR deployment, real-world disturbance events have revealed integration challenges, particularly those associated with transient behavior. In addition, interactions among power-electronics-enabled components may be difficult to identify before deployment, including the potential emergence of oscillations and sub-synchronous control interactions. High-frequency harmonics may also be amplified under specific system conditions and at particular network locations. The following real-world events and operational experiences provide some of the drivers for this work.

2.1.1 Unexpected Tripping During Disturbances

A series of large-scale incidents, including the 2016 Blue Cut Fire (NERC, 2017) and 2017 Canyon Fire (NERC, 2018) events in California and the repeated Odessa events in Texas in 2021 (NERC, 2021) and 2022 (NERC, 2022), have demonstrated how widespread fault-induced nuisance tripping and momentary cessation across multiple photovoltaic (PV) plants can cause rapid, large-scale generation loss. In each case, post-event analysis by the North American Electric Reliability Corporation (NERC) identified significant gaps in the availability of high-resolution, time-synchronized measurements from both plant and grid-side points of interconnection. As NERC reports, the unavailability of such data, in many cases, delayed the analysis of the root cause and identification of appropriate mitigation measures (NERC Alert

Level III, 2025). Subsequently NERC developed and approved PRC-029-2 Reliability Standard to address Frequency and Voltage Ride-through Requirements for Inverter-Based Resources (NERC, 2026).

2.1.2 Low-Frequency Oscillations and Sub-Synchronous Control Interactions

Recent incidents have also demonstrated that IBRs can introduce oscillatory behavior in the grid across a wide range of time scales, spanning from low-frequency forced oscillations to sub-synchronous control interactions (SSCIs). Examples include the 13 Hz and 5 Hz oscillations reported by Oklahoma Gas and Electric (OG&E) and Bonneville Power Administration (BPA), respectively, associated with type-3 and type-4 wind plants radially connected to series-compensated lines and the island-wide 18–20 Hz sub-synchronous oscillations (SSOs) on Hawaii's Kauai Island, which has multiple grid-following IBRs (Yunzhi, et al., 2022). While historically associated with wind farms connected through series-compensated transmission lines, SSCIs have also been observed in uncompensated and weak grids (Mulawarman & Mysore, 2011), such as the 4 Hz voltage-control oscillations reported by the Electric Reliability Council of Texas (ERCOT) and the 3.5 Hz real- and reactive-power oscillations in Hydro One in Ontario. A survey of many such SSOs from around the world can be found in (Yunzhi, et al., 2022). The reporting rate of PMUs imposes an inherent limitation on their effectiveness in monitoring high-frequency oscillations introduced by IBRs in the grid. In North America, most commercial PMUs have a reporting rate of 30 or 60 frames per second (fps) and hence, per the Nyquist-Shannon sampling theorem, oscillations higher than 15 or 30 Hz cannot be effectively analyzed.[1] A recent investigation of oscillations injected by solar plants conducted by Dominion Energy found that what appeared to be 8 Hz oscillations in 30 fps PMU measurements was actually the aliased component of 22 Hz oscillations injected by a solar plant (Wang, Mishra, Jones, Gardner, & Vanfrett, 2022).

IBR-driven oscillations have also been reported at lower frequency ranges. System operators with high levels of IBR deployment in their footprints like the California Independent System Operator (CAISO) have been reporting increased occurrences of forced oscillations that at times interact with inter-area modes and spread throughout electrical interconnections (Agrawal, Bohlen, Hiebert, & Penne, 2024). Communication failure at a BESS storage plant caused 0.25 Hz oscillations that interacted with a dominant inter-area mode (North-South A) in the Western Interconnection and were visible across the footprints of multiple system operators. CAISO was able to locate the source of oscillation by monitoring anomalous power output at IBR plants.

2.1.3 High Frequency Harmonics

Harmonic interactions have been observed in offshore wind plants connected to the grid through underground cables (Mueller, 2007). Such cables generally exhibit higher capacitance because of the close spacing between conductors, with the effect becoming more pronounced at higher transmission voltages. These interactions can be particularly significant under contingency conditions, highlighting the value of harmonic studies and appropriately designed filtering and mitigation measures. As additional power-electronic-based components, including large digital loads, are connected to the grid, filter designs and associated control settings may need to be reassessed and retuned to account for changing system characteristics. Accordingly,

[1] Formally, the Nyquist-Shannon sampling theorem applies to the process of sampling a continuous-time signal to create a discrete-time signal, and it does not directly extend to the reporting rate of phasor estimates computed from that signal. However, from a practical perspective, the parallels between a PMU's reporting rate and a signal's sampling rate are often straightforward to apply.

measurement bandwidths may also need to be appropriately configured to capture the relevant range of harmonic frequencies.

3.0 Monitoring Methods and Standards for an IBR-Rich Grid

No single measurement layer resolves all of the complexities of the modern power grid, so a practical monitoring approach relies on multiple measurement layers that serve different purposes and operate at different resolutions. This section discusses considerations for monitoring IBRs and provides a brief background on some of the related standards.

Monitoring location considerations are discussed in Section 3.1f., followed by methods and technologies for measuring IBR performance. Standards related to IBR performance monitoring are discussed in Section 3.2.

3.1 Monitoring Locations

IEEE 2800 (IEEE Std. 2800-2022, 2022) distinguishes between the point of measurement (POM), point of interconnection (POI), and reference point of applicability (RPA) for IBR performance requirements. As shown in the example in Figure 1, the POI is the electrical location where the IBR facility connects to the bulk power system (BPS), typically on the high-voltage side of the generator step-up transformer (GSU) at the transmission bus. The POM is where measurements are taken for compliance or operational monitoring. The POM typically coincides with the POI, but at times can also be separated from the POI by a short line interconnecting the plant to the transmission network. Depending on the configuration, the POM may also be located on the low-voltage side of the GSU or within collector circuits. The RPA is the point at which the ride-through and performance requirements are applied; this can vary based on facility configuration. For example, in a single large PV or wind plant with a dedicated POI, the default RPA is usually the POM or the POI. However, for a hybrid plant with multiple inverter groups or for aggregated distributed IBRs connected through a distribution network, the RPA may be upstream at a substation bus.

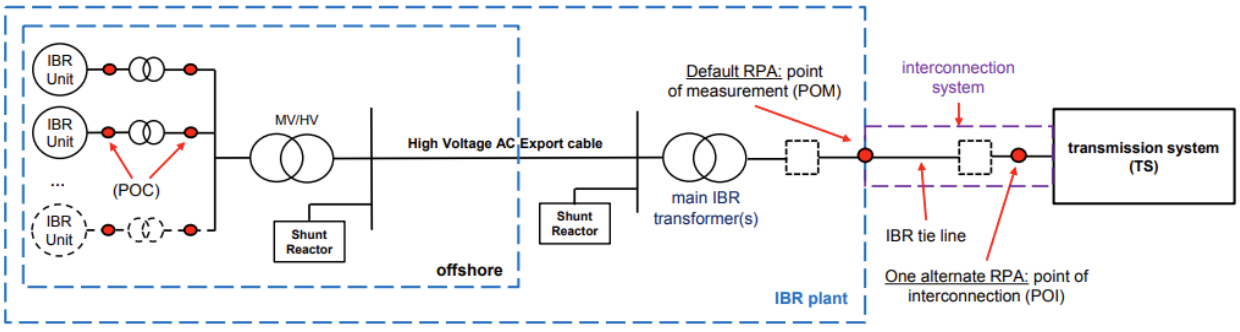


Figure 1. Schematic describing POM, POI, POC, and RPA. Adapted from (IEEE Std. 2800-2022, 2022).

Selecting the correct POM and understanding the RPA ensures that measured quantities truly reflect the IBR's compliance and operational performance as seen by the BPS, rather than being distorted by intermediate transformers, filters, or feeder impedance. For detailed information on the selection of POM and RPA based on the interconnection and configuration, please refer to Annex B of (IEEE Std. 2800-2022, 2022).

3.1.1 Types of Measurement Devices

A variety of monitoring methods are available to utilities and plant owners, and they are used for different purposes depending on the grid phenomenon of interest and the fidelity required to observe it. Common telemetered data sources include Supervisory Control and Data Acquisition (SCADA) and PMUs. SCADA typically provides one sample every several seconds, while PMUs provide time-synchronized measurements at much higher rates, commonly 30–60 reports per second. Devices that collect POW data operate at substantially higher reporting rates—typically 256 to 1,024 samples per second or faster—and capture the waveform directly rather than compressing it into phasor quantities. The following subsections discuss PMU and POW measurements in additional detail and provide examples of their appropriate use.

3.1.1.1 PMU-Based Monitoring of IBRs

PMUs are now the dominant technology for recording continuous high-resolution measurements in the power grid. PMUs estimate voltage and current phasors using digital samples of AC waveforms and produce synchrophasors synchronized to a common time source such as GPS. Typical reporting rates are 30 or 60 synchrophasors per second, which is suitable for capturing system dynamics and low-frequency oscillations and for enabling wide-area monitoring. Despite their limitations when it comes to monitoring fast IBR dynamics, PMU data can provide rich insights into the performance of these resources within the existing infrastructure that utilities have already deployed. PMUs estimate synchronized phasors and provide a wide-area picture of grid behavior, supporting low-frequency oscillation monitoring, phase angle monitoring, load monitoring, asset condition monitoring, and power plant model validation. These applications take advantage of synchronized measurements over a wide area, which is essential for real-time grid monitoring and stability assessment, and they benefit from mature deployment practices, standards, and protocols. The rest of this subsection discusses the advantages and appropriate use of PMU measurements for IBR monitoring through a series of examples.

Example 1: SCADA Data Versus PMU Data During Dynamic Events

A key advantage of PMU measurements is their ability to reveal dynamic behaviors that are not observable in slower telemetry like SCADA. One behind-the-meter solar farm example illustrates this contrast by comparing normal solar intermittency with sub-second events visible only in PMU (or waveform) measurements as shown in Figure 2. Over a ten-minute period, solar production fluctuated, largely due to intermittency, except for a single isolated drop that was not related to intermittency and was instead due to an abnormal solar inverter operation. The magnified view of this event, shown in Figure 2(b), indicates that this event lasted only a few hundred milliseconds. This was captured using micro-PMU (μPMU) measurements reported at 120 readings per second. A micro-PMU is a high-precision phasor measurement device designed for distribution networks, providing synchronized voltage and current phasor measurements with higher spatial resolution than conventional PMUs.

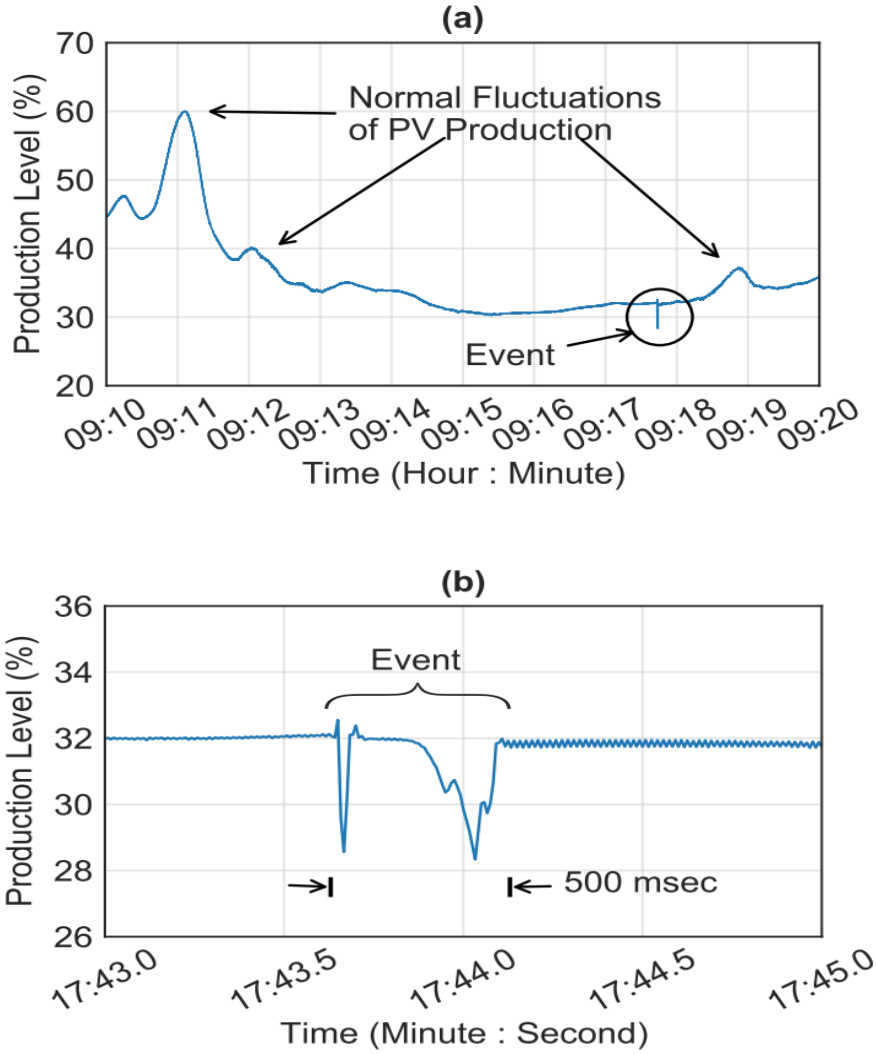


Figure 2. MicroPMU measurements at a 4.3-MW solar farm in Riverside, CA: (a) solar production monitored over a period of 10 minutes; (b) magnified view of an abnormal inverter operation at 9:17 minutes. Source: (Mohsenian-Rad & Khaledian, 2022).

The data is captured at a real-world setup of a 4.3-MW behind-the-meter solar farm in Riverside, California, shown in Figure 3, with one micro-PMU at the point of common coupling (PCC) and another micro-PMU on another feeder on the other side of the substation to serve as a reference.

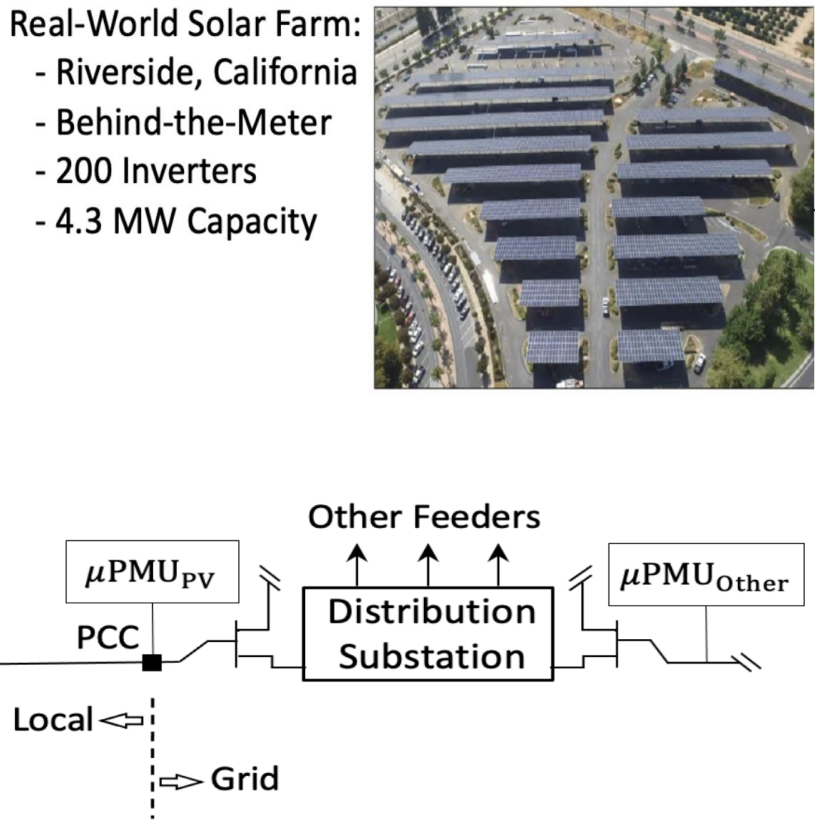


Figure 3. A microPMU monitor (μPMU_{PV}) is installed to track power fluctuations at the point of common coupling (PCC) of a 4.3-MW behind-the-meter solar farm in Riverside, CA. A second microPMU (μPMU_{Other}) is installed at the other side of the substation on another feeder as a reference. Source: (Mohsenian-Rad & Khaledian, 2022).

This type of observation underscores that IBR-relevant behaviors can occur on timescales that require higher resolution measurement than SCADA provides, and it demonstrates the practical value of PMU-based monitoring in identifying operational behaviors that might otherwise be missed. In particular, high-resolution monitoring of IBRs in microgrid or islanded grid environments can support the tuning of BESS control parameters for mitigating frequency deviations under renewable generation variability.

Example 2: Oscillation Monitoring with PMU Data

Another major PMU-supported application is oscillation monitoring, particularly because IBR controls span a wide time scale and may introduce oscillations across a wide range of frequencies. One useful way to characterize which oscillations can be reported with reasonable accuracy is through the Nyquist frequency, which is half the measurement reporting rate. In signal processing theory, frequency components below the Nyquist frequency can, in principle, be observed without ambiguity, while components above the Nyquist frequency will be aliased, meaning they fold into lower apparent frequencies and can be misinterpreted as slower oscillations. In the United States, transmission PMUs compliant with IEEE C37.118 standards typically report at 30 or 60 frames per second, corresponding to Nyquist frequencies of 15 Hz and 30 Hz, respectively, so oscillations below the Nyquist frequency should be observable with PMU data. However, due to filtering implementation within PMU hardware, estimation artifacts

may be introduced, and high-frequency oscillations may not be truthfully represented in PMU data even when they fall below the Nyquist frequency. (See (Chatterjee, et al., 2026) for a more detailed discussion.) Therefore, PMU data is best suited for analyzing oscillations below 5 Hz, where measurement fidelity is generally higher.

Oscillation monitoring solutions are available in several commercial wide-area monitoring platforms (Chatterjee, Biswas, Follum, & Kincic, 2023). These commercial tools are being utilized by system operators to detect and initiate mitigation actions when low-frequency oscillations appear in the system, potentially caused by IBR control actions (Purcell, Wold, Khan, & Bestebreur, 2025). In many cases, oscillation root cause investigations have helped identify IBR control parameter tuning issues, informing subsequent adjustments to mitigate similar oscillations in the future. Information from other monitoring resources such as SCADA is often utilized to augment gaps in PMU observability (Biswas & Follum, 2025; Agrawal, Bohlen, Hiebert, & Penne, 2024). Research-grade approaches have also been proposed that use phasor estimation at sub- and super-synchronous frequencies, rather than at the fundamental frequency, to identify the source of subsynchronous control interactions (Xie, Zhan, Shair, Ka, & Chang, 2019).

Additional examples of IBR-introduced oscillations that were detected and analyzed using PMU measurements are discussed in Section 4.7.

Example 3: IBR Model Validation with PMU Data

To preserve proprietary intellectual property, inverter vendors only share black-box models of inverter controls with system operators. Gaps exist in accurately representing inverters in positive sequence simulations, and phasor measurements can help calibrate IBR model parametrizations. Model validation and calibration using disturbance measurements playback has proved useful for improving the model quality of synchronous generators (Chen & Nayak, 2023; Biswas, Chatterjee, Follum, & Kincic, 2024) and holds immense potential for improving IBR models as well.

In literature, several research-grade algorithms have also been proposed for measurement-based validation and calibration of IBR models (Biswas, Tuffner, Follum, & Wall, 2024; Fan L. , et al., 2022; Etingov, et al., 2025). PMU measurements can also be used to validate whether IBR plants adhere to the frequency/voltage response obligations outlined in their interconnection agreements, serving as a useful screening for more detailed model-based analyses (Follum, Mana, Mitchell-Colgan, & Faris, 2025). Examples are provided in Section 5.3.

3.1.1.2 Point-on-Wave Measurement-Based Monitoring of IBRs

The need for richer observability is also tied to waveform fidelity. PMUs are well suited to capturing system dynamics, low-frequency oscillations, and wide-area situational awareness. However, a key limitation is that PMUs assume sinusoidal waveforms, which do not account for non-sinusoidal behavior that can occur with IBRs. In contrast, POW systems convert analog signals into digital samples that accurately reflect non-sinusoidal waveforms and therefore capture voltage and current waveforms at high sampling rates and preserves a much wider portion of the frequency spectrum. POW measurements are particularly well suited for detecting IBR behavior, which can vary significantly within a short span of time, and for capturing detailed system behavior that may be essential for diagnosing IBR performance. CPOW systems go further by providing either real-time streaming or continuously stored waveform data. While this high-fidelity data is well suited to the presence of IBRs and complex grid dynamics, it also

introduces practical challenges. The detailed nature of waveform data leads to significantly larger data volumes, requiring advanced data processing and storage solutions. Moreover, integration of POW systems into existing grid infrastructure and standards is still evolving.

Various tools and applications utilizing POW measurements are currently being developed and in some cases being deployed on the grid. These include tools for oscillation detection and localization using distributed applications (Biswas S. , et al., 2026), inertia monitoring (von Meier & Enas, 2025), and post-event IBR response evaluation (see the case study in Section 4.1). Given the data bandwidth limitation of POW applications, ongoing research and development is focused on developing solutions to perform more analytics at the substation, without the need for streaming POW data to the control center. Solutions include a broader set of distributed waveform analytics, in which POW measurements are recorded continuously and analyzed locally at or near the point of measurement. Under these approaches, high-resolution waveform measurements captured at sampling rates on the order of several thousand samples per second can be streamed to local analytics engines that perform real-time processing on site, eliminating the need to transmit raw waveform data to centralized servers (Lackner & Carroll, 2025). Applications of continuous POW include flicker detection and monitoring (Cooke, 2025) and advanced power quality assessment.

Using POW data in a synchronized manner across the grid is referred to as the synchro-waveform (Mohsenian-Rad, et al., 2024; Xu, Huang, Xie, & Li, 2022). The sensor device used to record synchro-waveforms is commonly referred to as a waveform measurement unit (WMU) (Halliday, 2018; Mohsenian-Rad H. , Smart Grid Sensors: Principles and Applications, 2022). WMUs record time-synchronized voltage or current waveforms at various locations across the power grid.

Compared to PMUs, which process raw data to compute and report phasor quantities, WMUs retain and transmit the raw waveform samples themselves. Like PMUs, WMUs achieve time synchronization through GPS or the Precision Time Protocol (PTP), making them a natural extension of conventional PMUs (Halliday, 2018). Time synchronization further enables IBR benchmarking for performance evaluation, by allowing a comparison of how different IBRs, whether from the same or different vendors, respond to the same disturbance events within a region. Such benchmarking can help identify anomalous IBR response or inconsistencies in control behavior.

Broadly speaking, IBR performance evaluation using synchro-waveforms can be divided into two categories: real-time monitoring and post-event analysis applications. Real-time IBR monitoring applications may include real-time detection of IBR-caused oscillations and instabilities (Yin, et al., 2025; Ehsani, Ahmadi-Gorjayi, Ye, McEachern, & Mohsenian-Rad, 2023), oscillation source identification and contributor ranking (Xu, Yong, Marquez, & Li, 2025), and harmonic distortion and power-quality monitoring of IBRs (Ahmadi-Gorjayi & Mohsenian-Rad, 2022). Post-event IBR analysis applications may include fault ride-through performance analysis (Yazdi, Li, & Mohsenian-Rad, 2025), oscillatory event forensics and remediation (Xu, Huang, Xie, & Li, 2022), condition monitoring and predictive diagnostics for inverters (Tong, Wang, & Zhao, 2025), benchmarking the responses of multiple IBRs to different types of disturbances in the power system (Mohsenian-Rad & Kezunovic, 2025), and data-driven IBR model validation and control parameter tuning (Ahmadi-Gorjayi & Mohsenian-Rad, 2023; Yazdi, Ahmadi-Gorjayi, & Mohsenian-Rad, 2025; Luo, 2023). Figure 4 gives an example of real measurements and playback signals for electromagnetic transient (EMT) model validation performed at ISO New England (Luo, 2023).

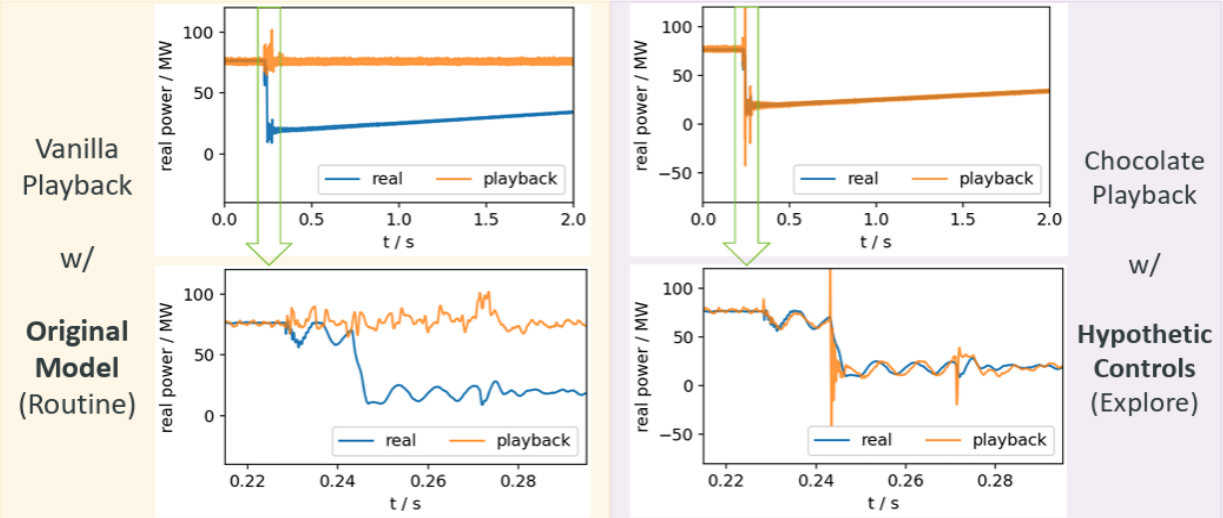


Figure 4. Inverter model calibration using measurement playback (Luo, 2023).

3.1.2 Continuous vs. Triggered Data Acquisition

The streaming and recording of PMU data is continuous at most U.S. utilities. However, for waveform data, the decisions on local storage versus continuous streaming depend on operational needs and communications bandwidth. At present the communication infrastructure in most utilities is not equipped to support continuous point-on-wave (POW) streaming. The practice is to record high-resolution waveform data locally, based on event triggers, and retrieve them manually as needed. The triggering settings, in this context, play a key role in determining the nature of the event that is being recorded. Conventional triggers are tuned to well-known signatures such as faults or oscillations; however, for IBRs, these may not encompass the full range of possible abnormal behaviors, underscoring the need to revisit and adapt triggering logic for inverter-driven phenomena.

3.2 Standards for IBR Performance Monitoring

This section reviews key standards governing data acquisition and telemetry relevant to IBR performance monitoring.

IEEE Standard 2800-2022 sets uniform technical minimum requirements for connecting large-scale solar, wind, and battery storage plants to transmission and sub-transmission power grids. It supports grid stability by dictating how IBRs handle faults, voltage changes, and system protection (IEEE Std. 2800-2022, 2022).

Post-mortem analyses of events such as the 2017 Blue Cut Fire, the 2019 Canyon Fire, the Odessa disturbance, and others in the United States have revealed that measurement data from IBRs were often inadequate for analyzing their dynamic behavior during these incidents. Drawing lessons from these experiences, NERC developed the reliability standard PRC-028-1 to define detailed monitoring requirements for IBRs, including measurement parameters, sensor types, reporting rates, data storage protocols, and data retention (NERC, 2025). The standard emphasizes that, in addition to phasor measurements, high-fidelity waveform recordings should be collected at the POMs of IBRs to enable comprehensive disturbance analysis. It applies to generator owners (GOs) and transmission owners (TOs) of IBR facilities that directly connect to

the BPS as well as any non-BPS IBR with a capacity exceeding 20 mega Volt Ampere (MVA) connected at 60 kV or higher.

PRC-028-1 specifies three main categories of measurements:

1. Sequence of Events Recording (SER): SER captures high-resolution status data that includes breaker operations and inverter-specific status indicators such as fault ride-through operations, mode changes, and control signals. These recordings provide critical time-stamped information on equipment operations and control responses during grid disturbances, supporting root-cause analysis and model validation.

2. Fault Recording (FR): FR consists of triggered, event-based waveform recordings that must capture phase-to-neutral voltages, phase currents (including neutral/residual currents), and real (P) and reactive (Q) power. Requirements specified in PRC-028-1 ensure that transient events are captured with sufficient detail to analyze fast dynamic behavior and equipment performance.

3. Dynamic Disturbance Recording (DDR): DDR requires continuous recordings of voltage and current phasors, real and reactive powers, and system frequency derived from the three-phase waveform measurements at the IBR POI. This continuous monitoring supports detailed analysis of system dynamics, including voltage and frequency swings, which are critical for understanding IBR performance during grid disturbances.

PRC-028-1 requires that all recording devices be time-synchronized to Coordinated Universal Time (UTC) via the GPS. Sensor placement is primarily at the POI, but the standard also recommends data capture at inverter terminals and along collector feeders to fully capture inverter response characteristics. Regarding data retention, all SER, FR, and DDR data must be accessible for a minimum of 20 calendar days from the date of recording.

Similar monitoring standards have also been established in Europe. The European Union's Network Code on Requirements for Generators (RfG) requires that Power Park Modules (PPMs) – a category that includes IBRs such as solar PV plants, wind farms, and BESS – support real-time or near-real-time communication and telemetry (ENTSO-E, 2026). While the RfG sets high-level obligations, specific telemetry requirements are further detailed in the European Network of Transmission System Operators for Electricity (ENTSO-E) guidance document (ENTSO-E, 2016) and are refined through national grid code implementations.

RfG classifies generator connections into types B, C, and D, based on connection voltage and installed capacity. This classification determines the applicable requirements for telemetry, control, and reactive power and ride-through capabilities. Larger units, such as Type D generators (typically above 75 MW in continental Europe and Great Britain), are subject to the most stringent obligations. Telemetry is expected for a range of dynamic and steady-state conditions, including fault ride-through events, grid disturbances, voltage and frequency deviations, and reactive power behavior. Generators must be capable of recording or contributing to data that captures their behavior during fault clearance, post-disturbance recovery, and other dynamic scenarios. The parameters to be communicated typically include active and reactive power output, voltage at the point of connection, frequency measurements and response status, control mode indicators and setpoints, and protection or fault conditions, including ride-through events. These capabilities are essential for Transmission System Operators (TSOs) and Distribution System Operators (DSOs) to monitor system behavior, verify

compliance, and coordinate operational responses, particularly under rapidly changing grid conditions.

4.0 IBR Monitoring and Analysis Case Studies

This chapter discusses real-world case studies that demonstrate how the monitoring approaches previously discussed are being applied to observe, diagnose, and interpret IBR performance. The case studies in Sections 4.1 through 4.6 were collected through questionnaires from IPRAM task force participants. The case studies in Section 4.7 describe IBR-introduced oscillations detected with PMU data as reported in various studies. The case study in Section 4.8 describes POW analysis of unexpected IBR responses to transient disturbances.

4.1 Dominion Energy Case Study

Dominion Energy has synchrophasor visibility across most of its transmission network using relays and digital fault recorders (DFRs) with PMU capabilities. DFRs sample at 4800 Hz, down-sampled to 960 Hz, and report a 30 Hz phasor component. Data is stored in the cloud-based PredictiveGrid™ platform for long-term access. Additionally, EPG's RTDMS and SEL's SynchroWave tools store PMU data on their own servers, but only for 30 and 14 days, respectively. The full architecture of this Synchrophasor Analysis Environment, as of March 2025, is shown in Figure 5.

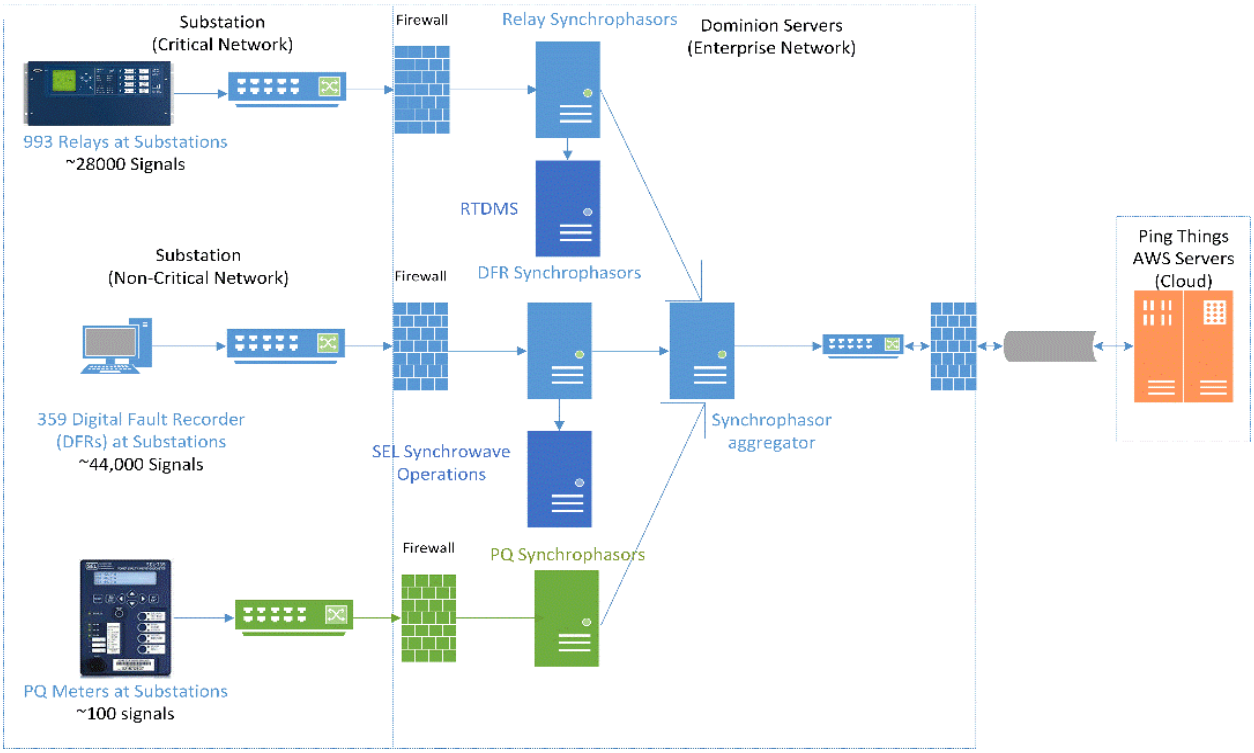


Figure 5. Simplified architecture of Synchrophasor Analysis Environment used by Dominion Energy to monitor its transmission network, March 2025.

4.1.1 Dynamic Performance Analysis of an Inverter-Based PV Plant During Sunrises and Sunset

This study investigates a recurring low-frequency dynamic behavior observed in a 105-MW PV plant, particularly during low irradiance periods around sunrise and sunset (Pudasaini, Vanfretti,

Mishra, De La Ree, & Jones, 2025). The plant, composed of 42 inverters and managed by a Power Plant Controller (PPC), exhibited oscillatory behavior in the reactive power output, triggering alarms in Dominion Energy's oscillation detection system. Power spectral density (PSD) analysis revealed a dominant frequency component around 0.07 Hz with harmonic peaks (Figure 6), indicative of nonlinear system dynamics. These oscillations were not present in the active power signal but were prominent in the reactive power, especially when the plant's output dropped below 1 MW. Time-frequency analysis using spectrograms (Figure 7) confirmed that these oscillations recur daily during low-power intervals, suggesting a systemic issue tied to the plant's control logic.

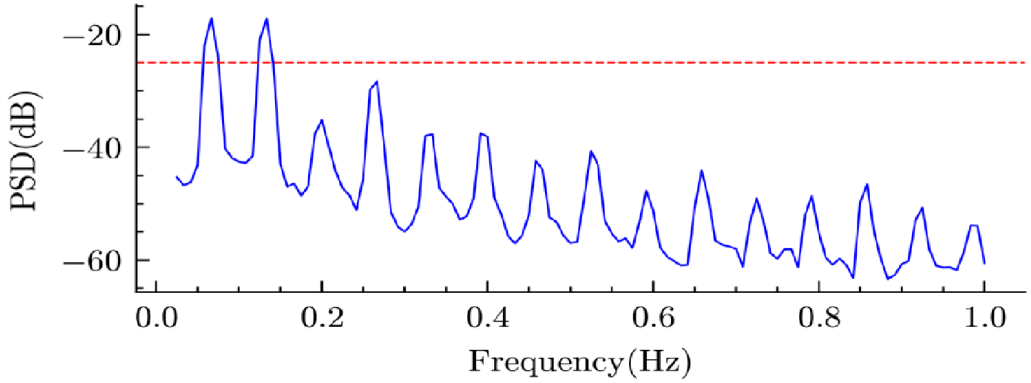


Figure 6. Power spectral density analysis of the current magnitude signal at the output of a 105-MW photovoltaic plant during the perceived oscillation, revealing multiple peaks.

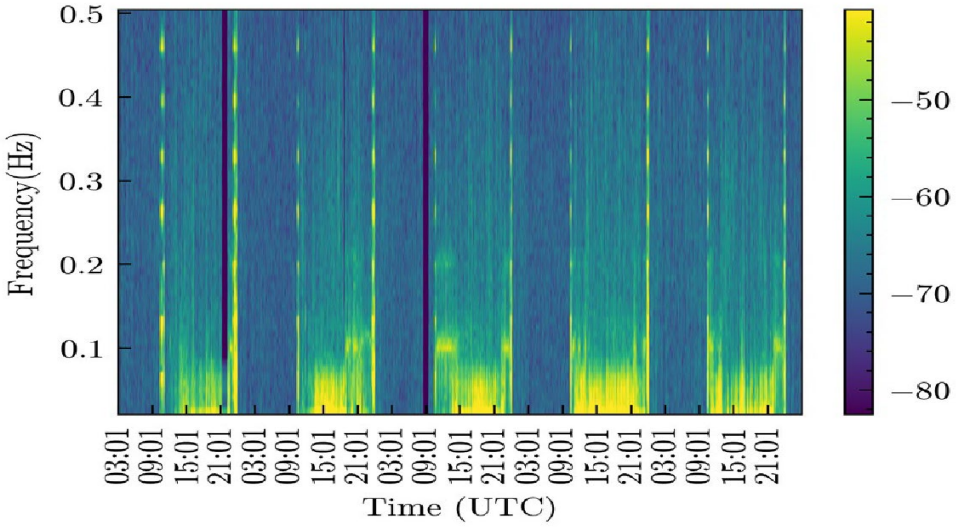


Figure 7. Spectrogram of the current magnitude signal at the output of the solar plant at a lower frequency range for five consecutive days.

The root cause was traced to the PPC's reactive power setpoint behavior and inverter transitions between operational modes under low DC input conditions. The inverters' attempts to maintain power factor within specified limits during minimal power output led to nonlinear reactive power fluctuations, misinterpreted as inter-area oscillations. This study highlights the need for improved coordination between PPC and inverter control strategies to prevent false alarms and ensure grid stability. It also highlights the use of Dominion's suite of measurement devices to analyze IBR performance and pinpoint specific issues.

4.1.2 Analyzing a Non-Sinusoidal Response from a Real-World Solar PV

There has been a recent increase in abnormal oscillations in Dominion Energy's power system stemming from unstable PV plant voltage controllers during outage season. This work (Mishra, Vanfretti, Delaree, & Jones, 2024) presents an analysis of an atypical, poorly damped slow (<0.05 Hz) response from a transmission-level PV solar power plant triggered by a local line outage in Dominion Energy's power system, shown in the top subplot of Figure 8. The uniqueness of this case resides in the fact that the plant's characteristic response is square wave-like, which was shown to not stem from conventional nonlinearities (such as control saturation). Furthermore, through a systematic investigation of PMU data at the POI, it was determined that the inverter dynamics played no role in characterizing this response and it was solely governed by the relatively simple PPC characteristics. Finally, using system identification (Figure 8, lower subplot), it was shown that the atypical nature stemmed from large feedback delays in the PPC.

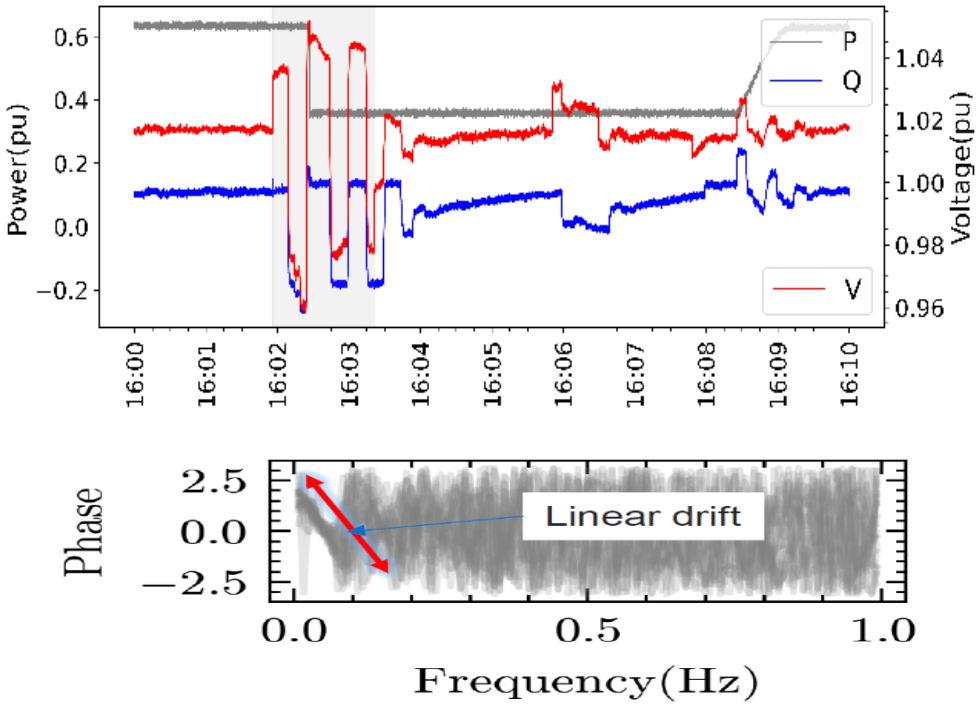


Figure 8. Analysis of an atypical, poorly damped slow (<0.05 Hz) response from a transmission-level PV solar power plant triggered by a local line outage in Dominion Energy's power system showing unique square wave response is not due to inverter dynamics but is due to large feedback delays in the PPC: Left - Square VAR Oscillations from PV; right - Feedback Delay Estimation using V-Q Causality.

Dominion Energy continues to use PMU data for post-event analysis, troubleshooting abnormal behavior, and identification of oscillation sources in the grid. The evolution of synchrophasor-based analytics has enabled Dominion Energy to adopt new processes and methods of grid management. With high visibility into grid dynamics through PMU data, the company has developed a deeper understanding of the complex behaviors of the grid, particularly as IBRs play a more significant role in grid operations. This has led to more informed decisions, ultimately ensuring a more reliable and resilient grid.

4.2 ISO New England Case Study

ISO New England (ISO-NE) actively uses PMU data to monitor IBRs' dynamic performance and their impact on the NE power grid. The applications running today are:

- Oscillation Detection and Characterization (OD&C),
- Oscillation Source Location (OSL),
- Automatic Power Plant Model Validation (APPMV), and
- Electromagnetic Transient Model Validation (EMTMV)

The first three applications are running online while the EMTMV is an offline application since it requires locally stored Point-on-wave (POW) data from devices like DFRs.

4.2.1 Oscillation Detection, Characterization and Source Location

As of October 2026, ISO-NE has completed the integration of key PMU data infrastructure into the CIP environment, including PDC, OD&C and OSL. Once OD&C detects an oscillation with operational impact, it will trigger OSL to determine the source (Maslennikov, Wang, & Litvinov, 2017). For oscillations originating outside NE, OSL will determine the direction of the source (e.g., from NY or NB side). For oscillations originating within NE, OSL will pinpoint the exact plant/generator. Alarms with key oscillation information will be sent to the EMS to enhance operator's situational awareness and support timely operational decision-making.

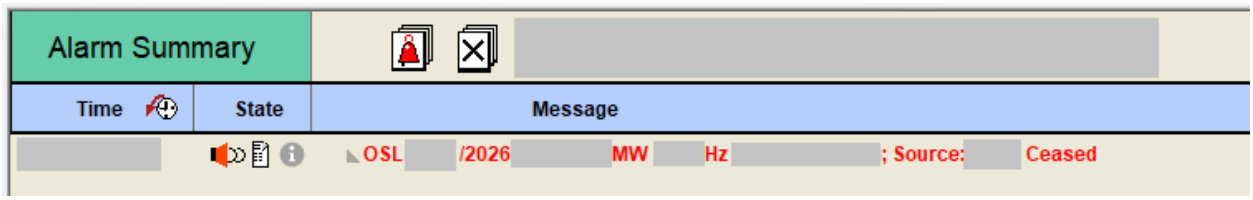


Figure 9. EMS Alarm Message Sample at ISO New England.

In parallel, an email with detailed information and analytical results will be automatically sent to real-time support engineers for verification and further investigation, as needed.

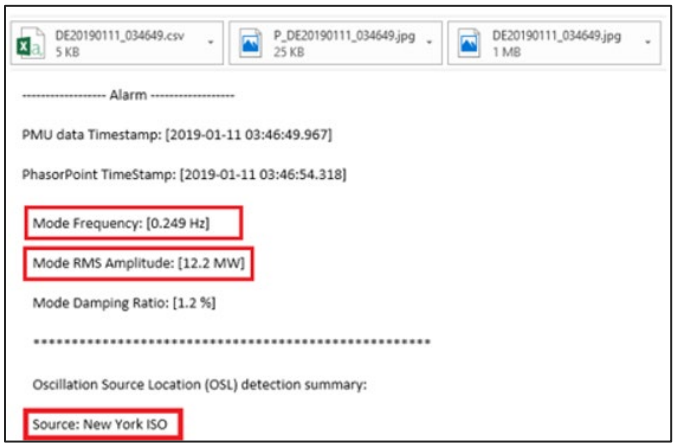


Figure 10. OSL Alarm Email Message Sample for the January 11, 2019, EI oscillatory event.

The OSL application has operated continuously in a fully automated online mode since 2017, well before the completion of the CIP project, providing real-time oscillation situational awareness and actionable source-location information to the real-time support engineers. Over the years, it has identified dozens of oscillation events with reliability impacts, many of which were traced to either equipment failures or improper control settings. These issues were subsequently investigated and resolved by the respective Generation Owners, improving both grid reliability and equipment performance. An example from a solar power plant is provided next.

A 0.15 Hz oscillation was detected by ISO-NE's OD&C and OSL systems in May 2024. The oscillation was first detected on the tie-lines between NE and NY, as depicted in Figure 11. Upon detection, the OSL application was triggered and identified a solar power plant in Maine, about 200 miles away from the NE-NY border, as the most likely source of the oscillation.

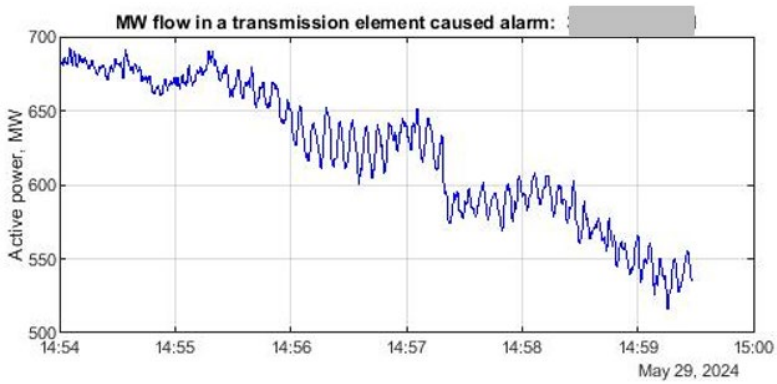


Figure 11. NE-NY tie-line flow for a 0.15 Hz oscillation originating in Maine.

As shown in Figure 12, the identified facility was located within a "suspect area" with limited PMU coverage containing multiple wind and solar power plants, making source identification particularly challenging. Nevertheless, OSL's pattern recognition algorithm (Maslennikov, 2024), leveraging both PMU and SCADA data (see Figure 13), successfully identified a specific solar power plant as the primary suspect and automatically sent out a detailed alarm email to real-time support engineers.

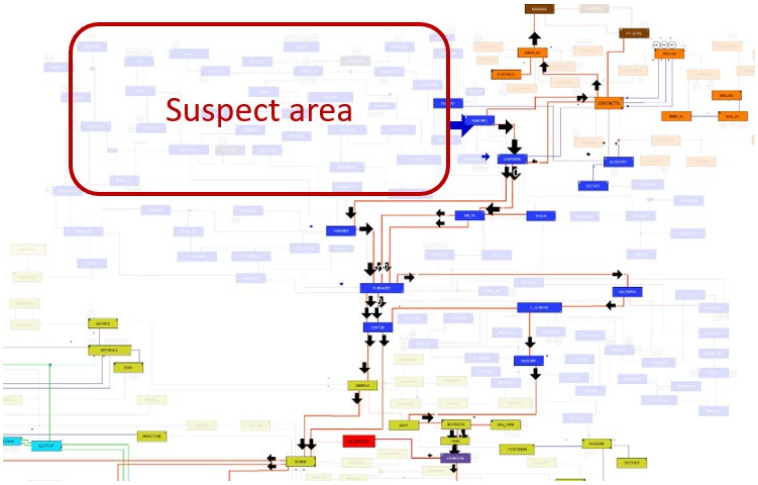


Figure 12. Dissipating energy flow plot on New England one-line diagram.

~~~ DE pattern recognition results
Source: Area=NEPEX (confidence=100%); station cannot be reasonably localized
Correlation between DE and DEtemplate with the highest rank is: 0.996

~~~ SCADA analysis results
Indices of MW and MVAR variability for generators

No	Station	Unit	MW_inde	MVAR_index
1	[redacted]	[redacted]	1	0.077
2	[redacted]	[redacted]	0	-
3	[redacted]	[redacted]	0.016	0.004
4	[redacted]	[redacted]	0.014	0.003
5	[redacted]	[redacted]	0.002	0.003
6	[redacted]	[redacted]	0.003	-
7	[redacted]	[redacted]	0	0
8	[redacted]	[redacted]	0	-
9	[redacted]	[redacted]	0.031	0.002

Figure 13. Analytical results from SCADA data.

Operations staff promptly reviewed the alarm, communicated with the suspected solar power plant, and received confirmation from the plant staff that the oscillation was originating from their facility. Fortunately, the oscillation damped out by itself after approximately 6 minutes.

Subsequent investigation determined that the root cause was the failure of a frequency control component within the plant's control system. Had the issue not been identified and corrected in a timely manner, it could have resulted in more severe impacts to both bulk system reliability and plant equipment. This event demonstrates the value of real-time oscillation detection and source-location capabilities in enabling rapid operator response and facilitating corrective actions by asset owners.

4.2.2 Power Plant Model Validation

Automatic Power Plant Model Validation (APPMV) and Electromagnetic Transient Model Validation (EMTMV) are complementary applications, validating both phasor models using PMU data (in APPMV) and EMT models using POW data (in EMTMV). APPMV operates automatically in an online environment, continuously validating the phasor models of power plants against actual grid disturbances. Isolated plant models, represented up to their POIs, are pre-configured within the application. When a significant system disturbance is detected, a PMU-data-driven playback simulation is automatically triggered in Powertech Labs' TSAT platform. As POW data becomes available, EMTMV will extend this capability to the validation of EMT models. Using a similar playback methodology in PSCAD, isolated plant EMT models up to their POIs will be validated against measured POW data to ensure that high-fidelity dynamic behavior is accurately represented.

Together, APPMV and EMTMV provide a comprehensive model validation framework spanning both phasor- and EMT-domains, helping ensure that planning and operational studies are based on models that accurately reflect field performance. An example of a solar plant ride-through event and the corresponding model validation results is shown previously in Figure 4.

4.3 ERCOT Case Study

ERCOT uses PMUs to monitor IBRs for ride-through events and oscillations. ERCOT currently has over 250 PMUs from three large TOs across the system streaming real-time data to ERCOT. Some PMUs are directly monitoring IBR facilities, but this is not uniformly the case. PMUs help ERCOT identify faults that coincide with the sudden loss of IBR generation. IBRs are

required to have PMU and DFR on site and ERCOT requests this information offline for event analysis. PMUs also help identify oscillations and the source of the oscillation is found with an in-house-built tool that searches through unit MW and MVAR telemetry to find and verify the source, which has often been from an IBR. The monitoring tools that are used include Electric Power Group's Real Time Dynamics Monitoring System (RTDMS) for real-time PMU data and the Phasor Grid Dynamics Analyzer (PGDA) for offline analysis. In case of an event, alarms from RTDMS are sent to PI applications to further help with event detection and analysis.

ERCOT continues to identify undesirable performance and work with Reliability Entities (REs), Generator Operators, and Qualified Scheduling Entities (QSEs) on a day-to-day basis to correct issues such as ride-through failures and oscillations. Some of the successful examples include correcting issues found in the Odessa events (NERC, 2021; NERC, 2022).

4.4 Bonneville Power Administration Case Study

Bonneville Power Administration (BPA) has been one of the early adopters of synchrophasor technology in the U.S. BPA contributions to the industry were recognized with its synchrophasor deployment project receiving S&P Global Platts Energy Award for Grid Optimization in 2013.

BPA successfully deployed Oscillation Detection application in its control room with real-time displays and operating procedures in place to guide dispatcher actions to mitigate grid oscillations and low damping conditions (Kosterev, et al., 2016). As shown in Figure 14, BPA detected events of sustained active and reactive power oscillations driven by inverter controls at a wind power plant with type-4 generators when the plant operated close to its full output. BPA worked with the plant owner and the inverter manufacturer to resolve the inverter control issues.

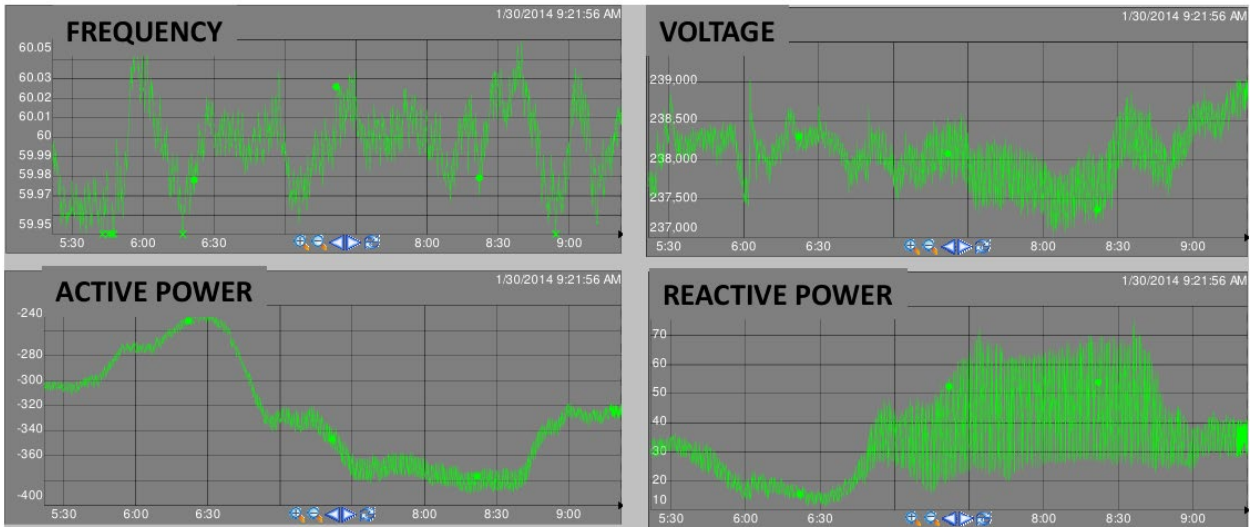


Figure 14. Control oscillation of an IBR plant at high power output.

BPA was one of the first Transmission Owners to require PMUs to be installed during interconnection of new generating resources, including IBRs. BPA Interconnection Standards require measurements at point of interconnection as well as medium voltage measurements and reactive devices. Today, BPA has PMUs monitoring 25 IBR plants with over 4 GW of total generating capacity. BPA recently deployed an application specifically monitoring oscillations at IBR sites.

BPA routinely uses PMU data for model validation of hydro power, thermal and IBR plants. Frequency deviation and reactive switching events are played in dynamic simulators to see whether the simulated performance of the plant matches observed responses. In example is provided in Figure 15. BPA will contact plant owners when persistent mismatches between the modeled and actual performance are observed. Below is an example of using PMU data for validation of a plant with inverter-based resources. Frequency and voltage are used as inputs, and active and reactive power as “measures of success” (Silverstein, Kosterev, Yang, & VanZandt, 2014).

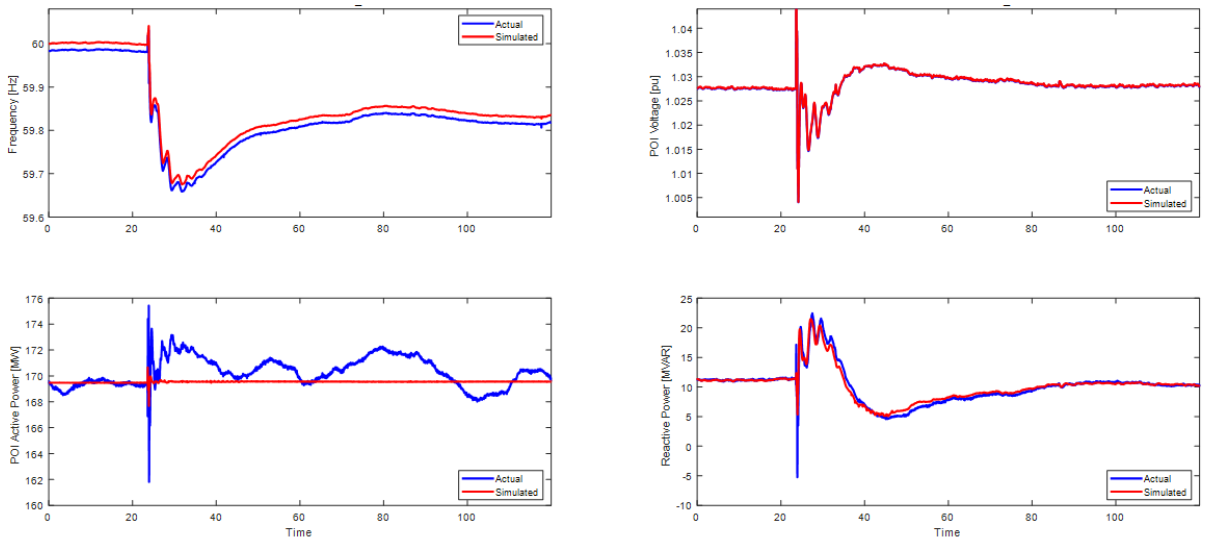


Figure 15. Disturbance-based model validation of an IBR plant.

4.5 COES ISO-Peru Case Study

The penetration of non-conventional renewable energy (solar and wind) in Peru currently reaches nearly 15% and is expected to increase to around 30% in the coming years. Although this percentage is still moderate, both solar and wind resources are concentrated in specific regions of the country. Solar generation, in particular, is mainly located in the southern region.

Many of the new solar plants entering operation are connected to a specific node: the San José 220-kV substation. This concentration of generation results in relatively low grid strength at that node. Figures 16 and 17 highlight the solar and wind potential in Peru, with the southern portion being a prime candidate for solar and the coastal and mountain areas being prime for wind.

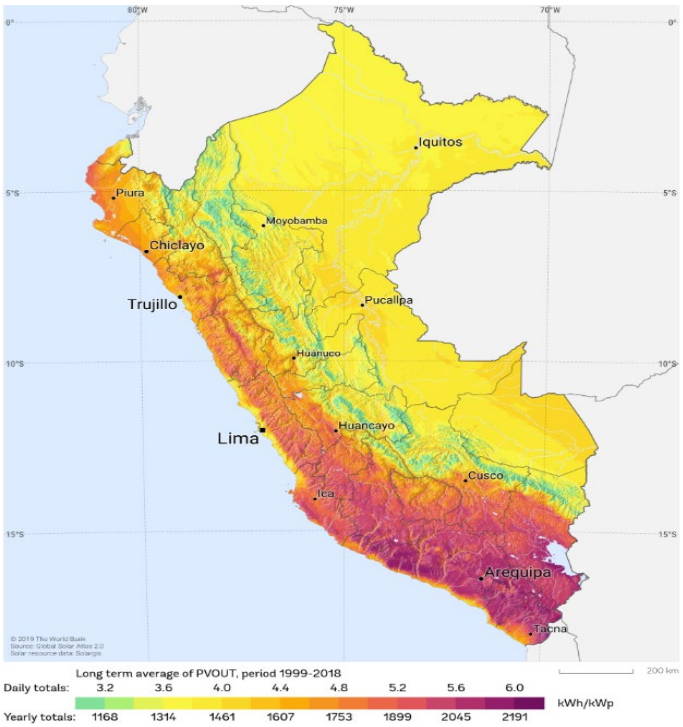


Figure 16. Solar potential and IBR concentration are predominantly located in southern Peru.

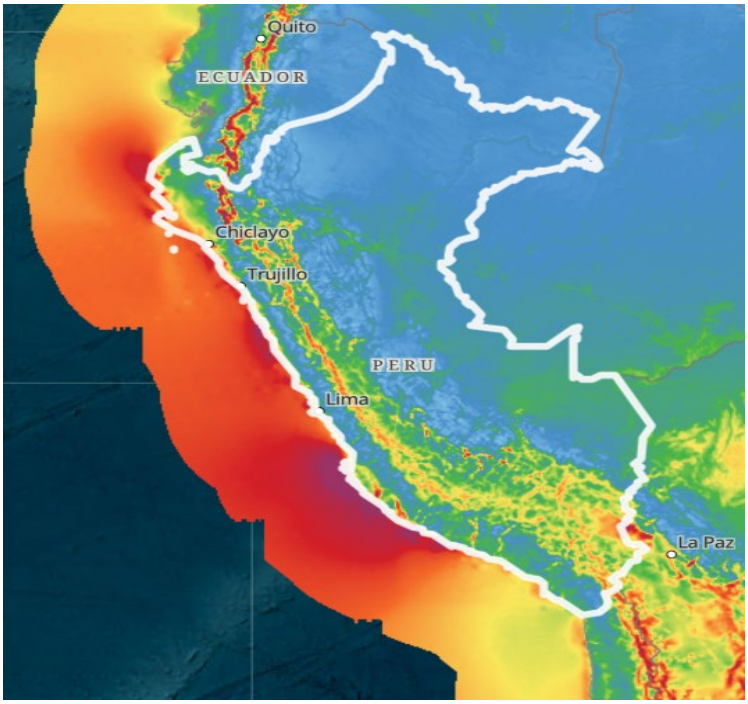


Figure 17. Wind potential in Peru is predominantly along the coast and the mountain ridges.

Historically, Peru's power system has been characterized by a strong presence of synchronous machines. Transitioning from a system dominated by synchronous generators to one with areas of high penetration of IBRs represents a significant paradigm shift. For many engineers who were trained primarily on the behavior and modeling of synchronous generators, this transition

introduces new technical challenges. In particular, there is an increasing need to undertake EMT studies; however, mandatory requirements for the provision of sufficiently detailed models to support consistent execution of such analyses are not currently in place.

In 2026, a national study is being developed to assess grid strength across the country and to identify which operational procedures and methodologies should be updated in order to define the need for new equipment. Under the current regulatory framework, mitigation measures that have been discussed, but have challenges for implementation, include curtailment of certain generators and installation of synchronous condensers to solve issues caused by the integration of new solar power plants.

Peru's Technical Procedure No. 20, "Connection, Modification, and Withdrawal of Installations in the Sistema Eléctrico Interconectado Nacional (SEIN)," establishes the requirements for the integration of power plants larger than 10 MW. According to this procedure, non-conventional generation plants must install a PMU at their point of connection.

In 2025, very low-frequency oscillations were detected due to the improper tuning of BESS units providing primary frequency response. The issue was resolved by retuning the controllers. The oscillations were identified using SCADA measurements combined with the methodology used to verify compliance with Primary Frequency Response (PFR) requirements. PMU measurements were not used in this case because the relevant installations were not equipped with PMUs.

In the future, all IBR installations are expected to include PMUs. These devices will support system monitoring, enable post-disturbance analysis, and help identify opportunities for operational improvements.

One of the main challenges is the interpretation of the signals and the implementation of appropriate corrective actions. Currently, there is no full EMT-compatible electrical model of the SEIN. While electromagnetic transient studies are often requested, they typically refer to traditional analyses such as energization studies and protection coordination. Models developed in ATPDraw generally do not include the detailed control models of IBRs provided by the manufacturers. Only recently have manufacturers been asked to provide black-box models to allow the analysis of weak-grid conditions and controller interactions using PSCAD, which is the official EMT simulation software used in the country.

At the San José 220-kV substation there is significant mining load, which is highly sensitive to voltage variations. Because this location also has excellent solar potential, many solar plants are connecting at this node. As is well known, phase-locked loops (PLLs) used in inverter controls are also sensitive to voltage disturbances. This makes it important to have higher monitoring of the system, especially in the parts of the grid more prone to voltage sensitivities.

In addition, a 350-MVA Static Var Compensator (SVC) is installed in the area. For this reason, detailed EMT studies and monitoring capabilities are required to ensure that no harmful controller interactions or weak-grid stability issues arise. This reinforces the role of high-resolution measurement devices in supporting system monitoring and event analysis in IBR-dominated grids.

4.6 Florida Power and Light Case Study

Florida Power and Light (FPL) is currently considering the use of PMUs and other monitoring capabilities for power system oscillation detection and source identification. Other areas of concern are IBR ride-through, transmission-level power quality issues and source identification.

Some of the challenges regarding the use of PMU data include storage and working with large datasets. When working with historical synchrophasor data in CSV format, the files can be in the range of several gigabytes (GB). Also, unless data is retrieved directly from the historian, sharing files among team members also creates challenges. FPL uses a combination of data for analysis. Complementing one another, FPL uses traditional historical SCADA telemetry and indication, dynamic disturbance recorders at several samples/cycle for POW data, digital fault recorders with much higher samples/cycle for POW data, and synchrophasor data.

4.7 IBR-Induced Oscillation Detected by PMU

The following subsections provide brief discussions of IBR-related oscillations detected by PMUs.

4.7.1 Battery-Induced Oscillations, California, January 2022

In January 2022, an instance of 0.25 Hz forced oscillations was introduced by a BESS plant in Southern California (see Figure 18) (Agrawal, Bohlen, Hiebert, & Penne, 2024). Since the oscillation frequency was close to the North-South A inter-area mode in the Western Interconnection, the oscillations were observed across multiple system operator footprints, and ~100 MW power swings were recorded on the California-Oregon Intertie (COI). The source of the oscillations was identified by RC West operators using PMU oscillation detection platforms in conjunction with SCADA displays of power plant outputs as well as calls to generator operators. This event challenged the prevailing assumption that IBR-induced oscillations are predominantly higher-frequency phenomena, demonstrating that much lower-frequency oscillations (e.g., ~0.25 Hz) can also be observed in practice.

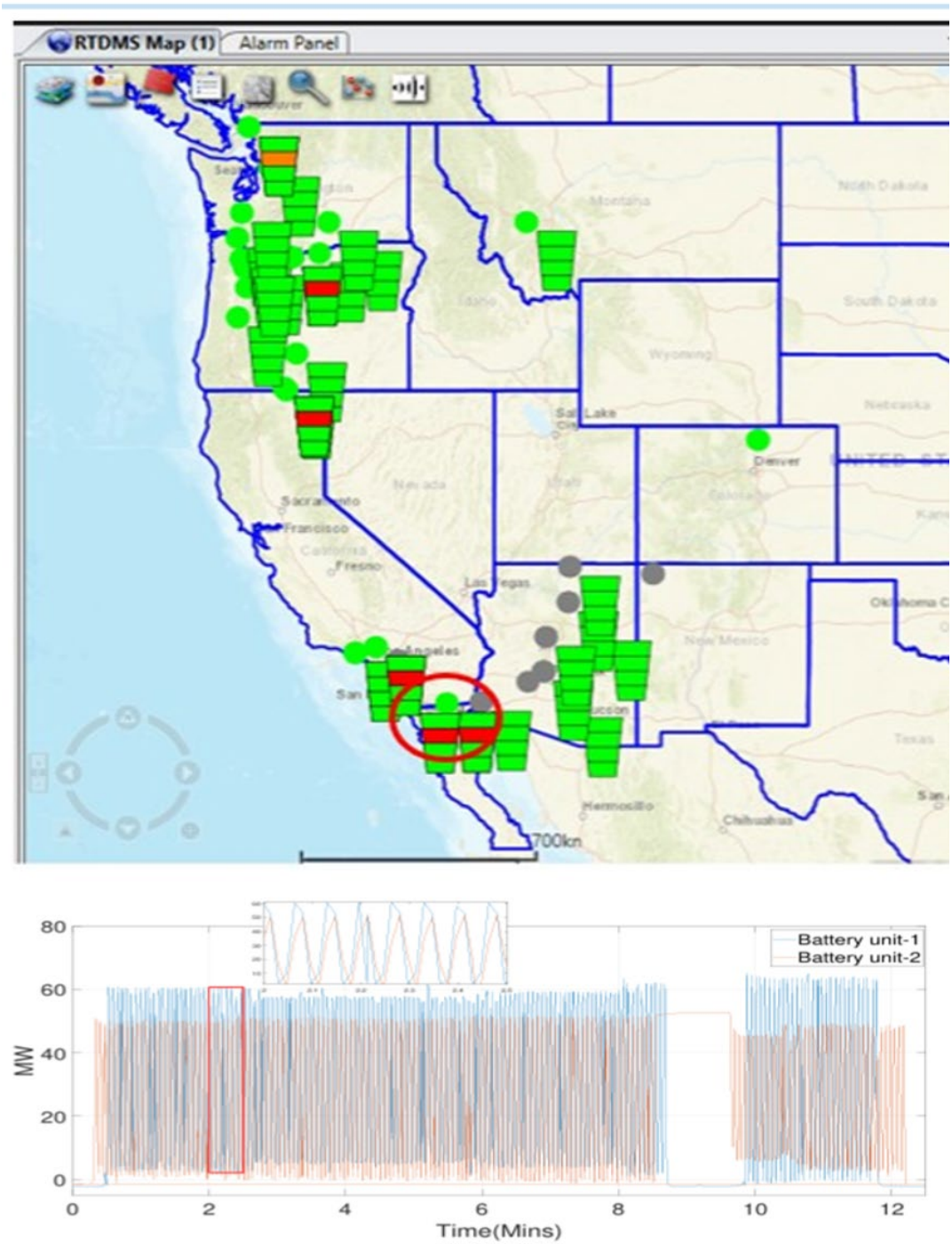


Figure 18. Lower frequency (0.25 Hz) oscillations introduced by telecommunication failures in a BESS plant in Southern California, January 2022 (Agrawal, Bohlen, Hiebert, & Penne, 2024).

4.7.2 Battery-Induced Oscillations, Arizona, 2023

Several forced oscillations observed in Arizona, also near 0.25 Hz, interacted with the inter-area North-South Mode A of the Western Interconnection (WI) and had wide-area observability (Rhodes & and Goodrich, 2024). PMU data helped initiate root-cause investigations that

identified operating-point-dependent limitations in plant-control parameter tuning that led to the oscillations. Further details on the root causes are provided in Table 1.

Table 1. Root cause investigation results for several IBR-induced oscillations observed in the Salt River Project (SRP) territory and their Western Electricity Coordinating Council (WECC) impact (Rhodes & and Goodrich, 2024).

Date	Root Cause
9/20/2023	Error in metering loss compensation methodology (Divided by zero)
11/02/2023	Differences in start-up timing across GSUs GSU-level inverter setpoint polarity inversion
11/03/2023	PV output hardcoded to 0 for testing (not actual PV output) leading to meter switching logic error

4.7.3 Battery-Induced Oscillations, Cordova, Alaska

MicroPMUs installed in an island power system in Cordova, Alaska, were instrumental in establishing a correlation between BESS operating conditions and the appearance of an oscillation (Becejac, Follum, Vartanian, & Cain, 2020). The utility worked with the BESS vendor to tune the synthetic inertia settings of the inverter and reduced the magnitude of the observed oscillations. A sample set of observed oscillations is shown in Figure 19.

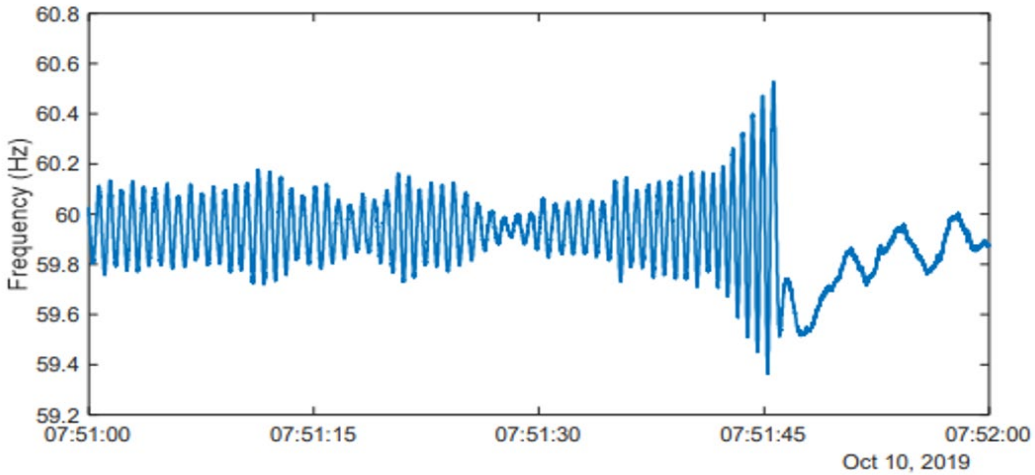


Figure 19. MicroPMU measurements detect oscillations in an island power system in Cordova, Alaska, due to a battery energy storage system (BESS) (Becejac, Follum, Vartanian, & Cain, 2020).

4.7.4 18-20 Hz IBR-Induced Oscillations, Kaua‘i Island, Hawaii, November 2021

IBR-induced oscillations of 18 to 20 Hz were observed in the 57-kV transmission network of the Kauai Island power system. Post-event model- and measurement-based diagnostics revealed several mitigations for the observed oscillations, such as the retuning of IBR phase-locked loop

(PLL) and frequency-droop settings (Dong, et al., 2023). The local utility was able to mitigate the oscillations by changing the control mode of one of the IBR plants from grid-following to grid-forming.

4.8 Point-on-Wave Analysis of Unexpected IBR Responses to Transient Disturbances

The following example was published in (Yazdi, Li, & Mohsenian-Rad, 2025), where real-world synchro-waveform data from 68 IBRs were investigated during a 500-kV fault in Ontario, Canada. The waveform measurements had a resolution of 128 samples per cycle. The locations of the IBRs and the fault are shown in Figure 20. For each IBR, the color denotes the class of the IBR's waveform response. These classes are identified by applying pattern recognition on synchro-waveform measurements:

- Class 1) The IBR trips during the fault.
- Class 2) The IBR trips after the fault is cleared.
- Class 3) The IBR rides through the fault, supplying some fault current.
- Class 4) The IBR exhibits a short-lasting (momentary) reduction in power injection.
- Class 5) The IBR exhibits a long-lasting reduction in power injection.
- Class 6) The IBR experiences sub-synchronous oscillations.
- Class 7) The IBR exhibits prolonged high current for many cycles after the fault is cleared.

Representative examples for the waveform response in each class are shown in Figure 21.

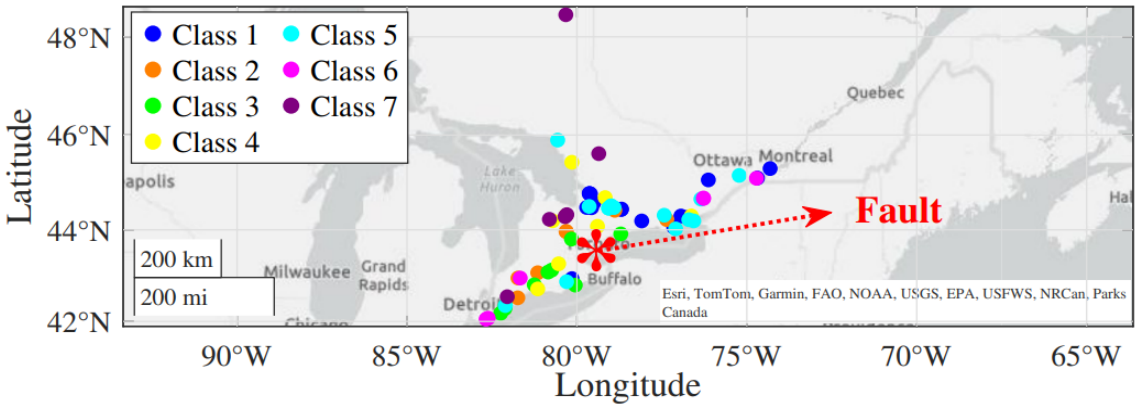


Figure 20. The locations of 68 IBRs with WMUs in Ontario, Canada, whose waveform responses to a system-wide disturbance caused by a 500-kV fault was studied in (Yazdi, Li, & Mohsenian-Rad, 2025).

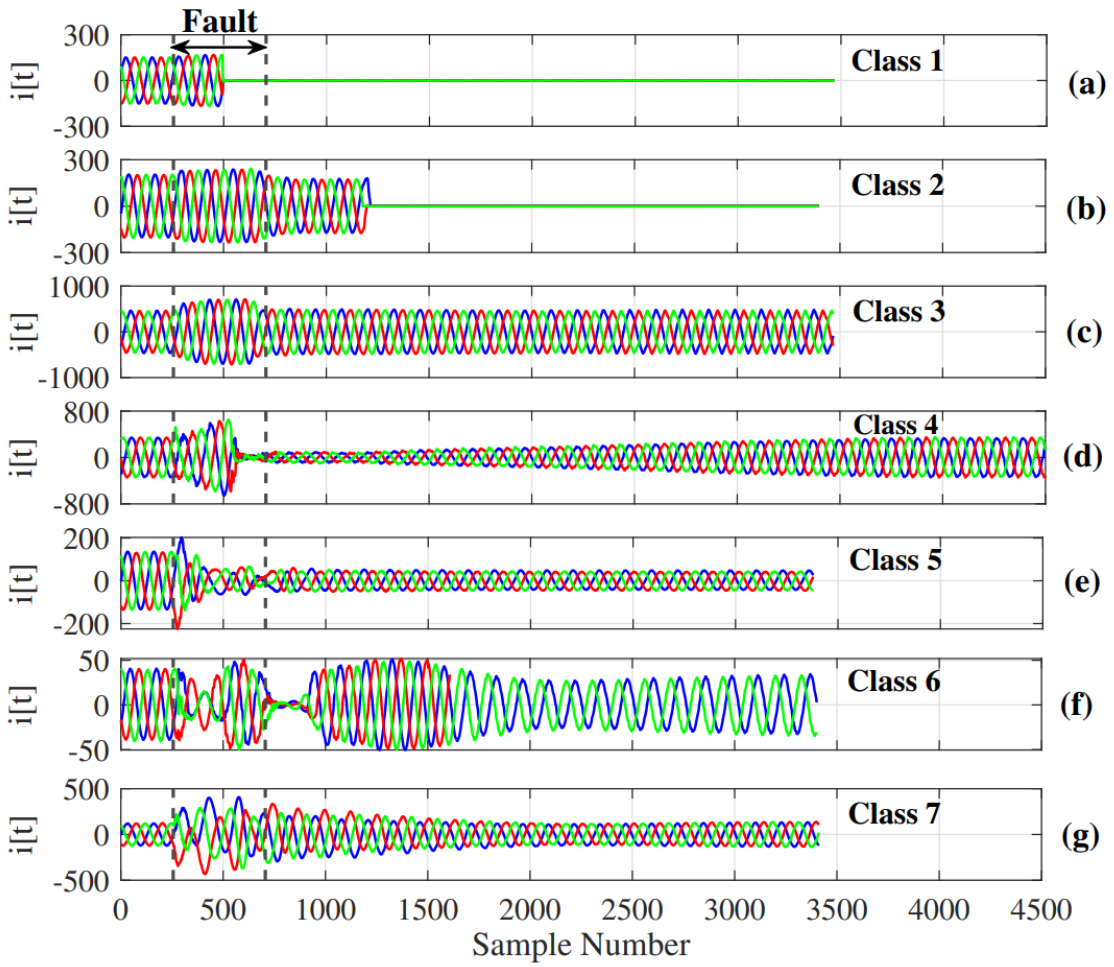


Figure 21. Examples of the current waveforms for the IBR responses in each of 7 classes identified by applying pattern recognition on synchro waveform measurements. Source: (Yazdi, Li, & Mohsenian-Rad, 2025).

Detailed discussions about the characteristics of the waveform responses in each class, as well as the lessons learned from the analysis of synchro-waveforms, are available in (Yazdi, Li, & Mohsenian-Rad, 2025). Specifically, the analysis addressed:

1. Sudden versus oscillatory tripping in Class 1: Three IBRs, all in Class 1, experienced high-frequency oscillations during the fault. In other words, a subset of the responses in Class 1 experienced oscillations while the rest of the responses in Class 1 did not experience oscillations.

2. Sub-synchronous oscillations: Six IBRs, all in Class 6, experienced sub-synchronous oscillations, i.e., at frequencies below the fundamental frequency and often with sideband frequencies. The available data are sufficient to detect the presence of sub-synchronous oscillations; such as in Figure 14(f). However, the available data is not sufficient to fully characterize them. This is because some WMUs record only a few cycles after the disturbance. Due to the low frequency of sub-synchronous oscillations, we need waveform data over longer periods. Using continuous (i.e., gapless recording of) waveform measurements would resolve this shortcoming.

3. Partial tripping in IBRs with multiple inverters: The IBRs in Class 5 had a long-lasting reduction in power injection; see the example in Figure 14(e). The utility records revealed that all IBRs in this class have multiple inverters and they experienced partial tripping, where a subset of inverters tripped. Tripped inverters had Class 1 or Class 2 responses. Inverters that did not trip had Class 3 responses. However, since the waveform measurements are collected at each IBR's interconnection point, the overall response is in Class 5.

4. Timing of tripping and distance from the fault location: Both Class 1 and Class 2 involve tripping. The timing of tripping significantly varies even within the same class. The IBRs in Class 1 are between 78 km to 455 km away from the location of the fault. However, the farthest IBR in Class 2 is 220 km from the fault, which is less than half of the farthest IBR in Class 1.

5. Causes of post-fault tripping: IBRs in Class 2 trip after the fault is cleared. The circumstances of a post-fault tripping were investigated by zooming in and analyzing the voltage and current waveform measurements after the fault was cleared. In some cases, we could observe that the cause of tripping after the fault was due to post-fault voltage distortions at the IBR terminals.

6. Geographical patterns: Recall from Figure 13 that the colors on the map denote the classes of the IBRs. Some geographical patterns can be identified in this figure. Almost all IBRs in Class 1 are on the north and north-east side of the fault location. Almost all IBRs in Class 3 are on the west side of the fault location. Almost all IBRs in Class 7 are on the north side of the fault. The IBRs in Classes 2, 4, 5, and 6 are geographically scattered across the region with no pattern.

7. Analysis of the types of resources: Almost all IBRs in Classes 1 and 5 are solar generation resources. The rest of the classes include both solar and wind IBRs. Classes 2 and 7 have more wind than solar IBRs. Classes 3, 4, and 6 have more solar than wind IBRs. Class 7 maintains a high current even after the fault is cleared. This is likely due to internal dynamics in the IBRs in this class. All other classes stop supplying fault current once the fault is cleared.

The study by (Yazdi, Li, & Mohsenian-Rad, 2025) also developed analytical methods to assist system operators to identify which IBRs demonstrate abnormal behavior, in comparison with comparable IBRs, in terms of metrics such as IBR type, geographical location, voltage level, etc. This is one example of the use of POW data for detailed IBR performance assessment post-event.

5.0 IBR Performance Monitoring and Analytics - Proposed Advanced Methods

The preceding sections established the motivation for IBR performance monitoring, reviewed existing and demonstrated monitoring approaches, and presented real-world case studies that illustrate how these techniques are being applied in practice. Building on that foundation, this chapter focuses on three emerging methods that provide solutions for deeper analysis, evaluation, and prediction of IBR performance. Section 5.1 presents interharmonics-based IBR oscillation monitoring, which offers solutions for identifying and characterizing oscillatory behavior. Section 5.2 discusses modeling and prediction of IBR dynamic response, reflecting the broader goal of using measurement-driven insight not only to observe behavior but also to anticipate it. Section 5.3 describes a structured means of evaluating and comparing the performance of individual generation resources in response to system events.

5.1 Interharmonics-Based IBR Oscillation Monitoring

IBR-caused power system oscillations or small-disturbance stability issues have been a concern in the industry due to increased oscillation incidents. Oscillations are traditionally investigated using phasor data such as those recorded by PMUs. In a recent development, the waveforms underlying the phasor oscillations are examined (Xu, Yong, Marquez, & Li, 2025). It was found that the existence of a type of spectral components called interharmonics is the necessary and sufficient condition of phasor oscillation. The finding has led to some new and effective strategies for oscillation monitoring and analysis. This subsection explains this development and one of the resulting applications – a new method for oscillation source location. This is especially useful in monitoring systems with significant IBR penetration.

5.1.1 Interharmonics Causing Phasor Oscillation

Figure 22(a) shows the measured current waveform associated with a wind farm's oscillation event. If one performs Fourier analysis on the waveform, a spectral component at 63.5 Hz can be seen (Figure 22(b)). There is also a smaller component at 56.5 Hz. These are interharmonic components per IEC 61000-4-30 (IEC 61000-4-30, 2015). The standard defines interharmonics as the spectral components that reside between harmonic frequencies. For convenience, interharmonics here refer to both components below and above the fundamental frequency. Interharmonics are also called non-integer harmonics in some literature.

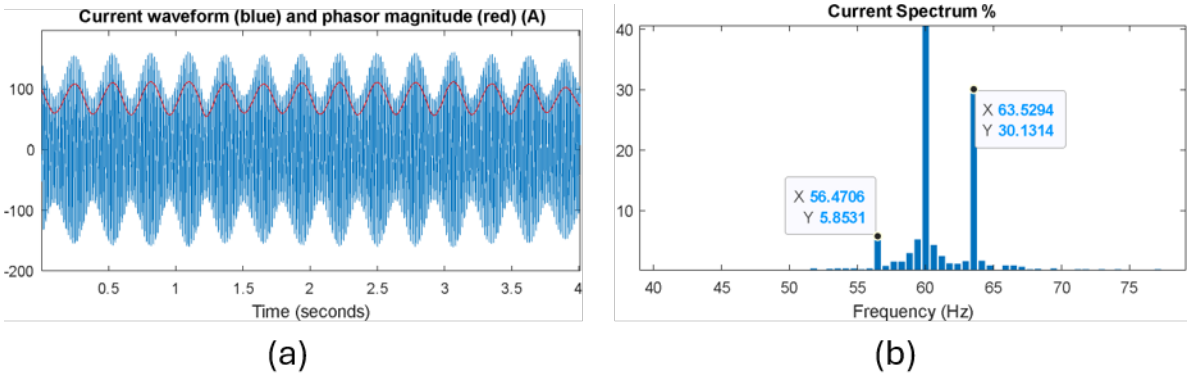


Figure 22. Sample time-domain waveform (a) and frequency-domain spectrum (b) of phase A current of a windfarm.

The mechanism through which interharmonics cause phasor oscillations can be understood intuitively by examining a waveform that contains one interharmonic component as follows:

$$v(t) = v_1(t) + v_{ih}(t) = \sqrt{2}V_1 \sin(2\pi f_1 t) + m\sqrt{2}V_1 \sin(2\pi f_{IH} t + \varphi_{IH})$$

where m represents the percentage magnitude of the interharmonic component with respect to the fundamental frequency component. Figure 23 shows the example waveforms of $v_1(t)$, $v_{ih}(t)$, $v(t)$, and the magnitude of resulting phasor. The phasor associated with the k^{th} cycle of voltage $v(t)$ is calculated using the PMU algorithm as follows (IEEE Std C37.118.1-2011, 2011):

$$(V)_{phasor}(k) = \frac{1}{\sqrt{2}T_1} \int_{(k-1)T_1}^{kT_1} v(t) e^{(-j2\pi f_1 t)dt}.$$

The magnitude of the above phasor is essentially the root mean square (RMS) value of $v(t)$ in the k^{th} cycle. It can be seen from Figure 23 that peaks of $v_{ih}(t)$ are not synchronized with those of $v_1(t)$. As a result, the two peaks add at cycle A but subtract at cycle B. Thus, the RMS value or the magnitude of the phasor of cycle A is larger than that of cycle B, leading to the appearance of phasor oscillation. This is the well-known wave beating phenomenon created when two waves of different frequencies interact with each other. The beat frequency equals the phasor oscillation frequency. It is useful to note that if $v_{ih}(t)$ has a harmonic frequency, the phasor will not oscillate since the peaks of harmonic components are synchronized with fundamental frequency.

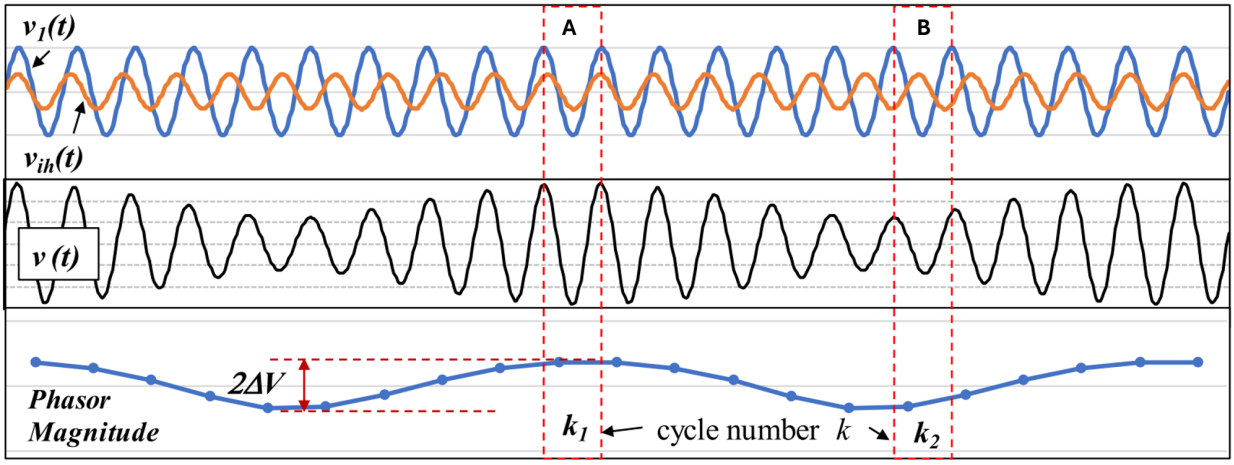


Figure 23. Mechanism of an interharmonic causing phasor oscillation.

The concept of interharmonics may be new to phasor-based stability or oscillation investigators, but it is well known in the field of power quality (IEEE Std 1453-2015, 2015). For example, interharmonics are a known cause of voltage flicker (Tayjasanant & Xu, 2004). The phasor of flickering voltage also exhibits a steady oscillation or beating pattern. From the perspective of power system oscillation or small-disturbance stability, two common sources of interharmonics are:

- Generation of interharmonics by synchronous generators and IBRs. For example, it has been shown that the oscillation of a synchronous generator's rotor will produce interharmonic voltages at the generator's terminal instead of an oscillating phasor angle as commonly taught (Xu, Yong, Marquez, & Li, 2025).

- Natural frequencies of a circuit: with the combination of line inductor (L) and capacitor (C) components on a circuit creates a natural resonant frequency inherent to the grid's architecture, which can be characterized using the eigenvalues of the circuit. It is unlikely that these frequencies are integer multiples of the fundamental frequency (60 Hz or 50 Hz). As such, the natural frequencies are interharmonic components. The real part (σ) of a complex eigenvalue ($\lambda = \sigma \pm j\omega$) determines the damping of that specific natural frequency mode. If the circuit possesses a negative damping characteristic, i.e., if one of such components has an eigenvalue with a positive real part ($\sigma > 0$), instead of decaying after a transient disturbance, the interharmonic component extracts energy from the system and grows exponentially over time, which will result in growing phasor oscillation.

The interharmonic finding has many potential applications. One of them is to locate the sources causing an oscillation event. The idea is very simple and can be explained as follows:

- Phasor oscillation means there are interharmonics in the underlying voltages and current waveforms.
- Powers at the interharmonic frequencies are needed to drive the propagation of the interharmonic voltages and currents in the system.
- Therefore, interharmonic power producers are sources causing oscillations.
- By checking the amount of interharmonic power produced by various components, we can locate the oscillation sources and rank their impact.

The above monitoring scheme can be implemented easily and is explained below. In Figure 24, waveform (or interharmonic power) monitors are placed at the interface points of power plants and the grid. The interharmonic powers entering into the grid are extracted to determine if a power plant is a source contributing to an oscillation event. The simplest version of the data processing algorithm is as follows:

- Use the degree of fluctuation of the RMS (or phasor) current as the trigger to start capturing oscillation events. Note that currents are more sensitive to oscillation than voltages.
- Perform DFT on the captured waveform data by using a window size that covers one oscillating (i.e., beating) period of the waveform.
- Calculate three-phase active powers for the interharmonics of interest, one data window by one data window.
- Optionally, compute the average powers over the entire duration of the oscillation event. The average power is proportional to the interharmonic energy produced. It can measure the total effect of interharmonic power generation or consumption over the event.
- Compare the interharmonic powers of all monitored plants obtained for the same period of interest. Based on the amount of power and/or energy generated, determine if a plant is a contributing source and its degree of contribution to the oscillation event.

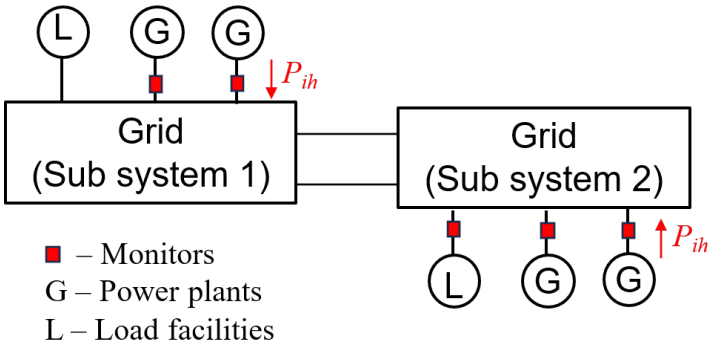


Figure 24. Scheme for oscillation monitoring and source location.

There are other versions of implementation. Examples are 1) Individual generators in a power plant can be monitored to determine if a specific generator is the source, and 2) Interharmonic powers flowing in the interface lines between two subsystems can be monitored. The total interharmonic power across the interface can indicate if an area is the net contributor to an oscillation event. It is useful to note that waveform recording devices in the form of power quality monitors are already available for all types of power plants per standards such as IEEE Standard 2800 (IEEE Std. 2800-2022, 2022). Such devices do monitor interharmonics per IEC 61000-4-30 from the perspective of power quality compliance. Modern versions of these monitors can provide synchronized waveform data as well (Xu, Huang, Xie, & Li, 2022). These devices inherently capture the raw frequency data needed. Adding the source location algorithm transforms these compliance tools into a diagnostic instrument.

5.1.2 Field Examples of Oscillation Source Location

Two examples of applying the interharmonic power idea to locate oscillation sources are presented in this section. For both cases, power quality monitors recorded the beating waveforms.

5.1.2.1 Case of Wind Farms

The first case involves several wind farms shown in Figure 25. The opening of Breaker B triggers an unstable oscillation in the area due to increased impedances between the wind farms and the grid (Li & Reinmuller, 2019). Adequate data is available for wind farms WF2 and WF3. The goal here is to determine which farms contribute more to the oscillation event.

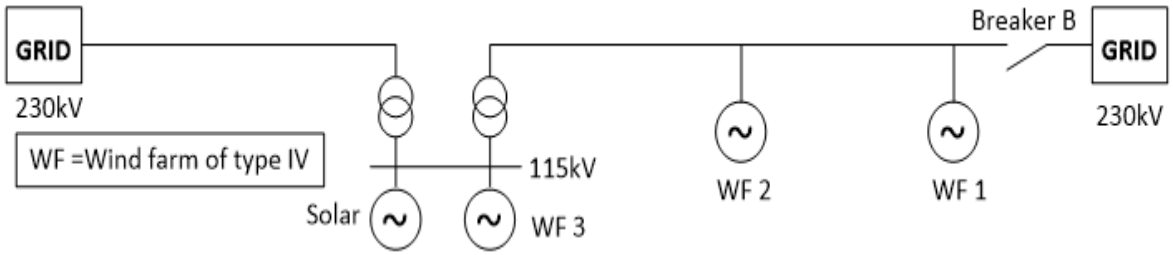


Figure 25. A case of windfarm oscillations.

Figure 26 shows the waveform and its spectrum of phase A current of WF3. The main interharmonic component is the one at 63.5 Hz. The results associated with WF2 have been shown in Figure 22. The main interharmonic component is also at 63.5 Hz.

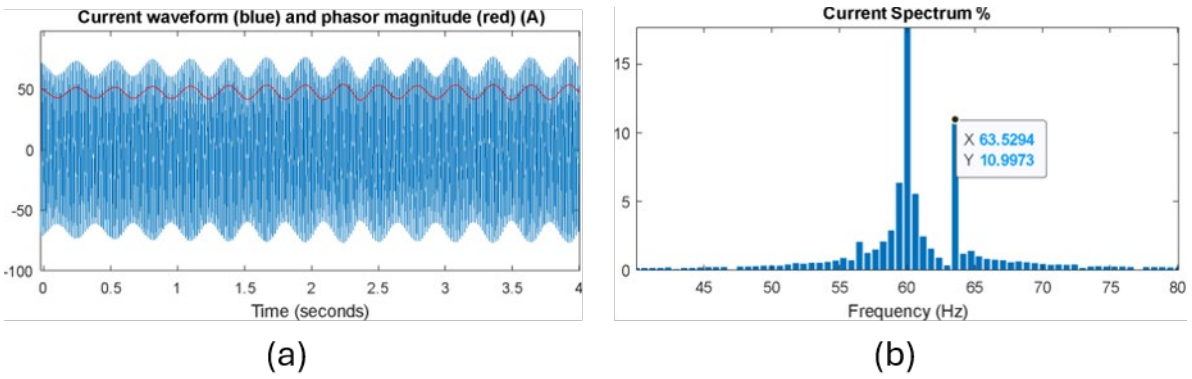


Figure 26. Sample time-domain waveform (a) and frequency-domain spectrum (b) of phase A current of WF3.

The interharmonic power injected into the grid at WF2 and WF3 locations are shown in Figure 27. Each bar of the chart represents the result obtained for one oscillation period. Since there are 14 oscillation periods in the 4 seconds of data, there are 14 sets of bars. The frequency of oscillation is about 3.5 Hz (=14/4). It can be seen that both wind farms are injecting interharmonic power into the grid. Therefore, both contribute to the oscillation event and can be called sources. WF2's power is much larger, so it is the larger contributor. Note that other power plants in the system (unanalyzed here) can also be contributing sources.

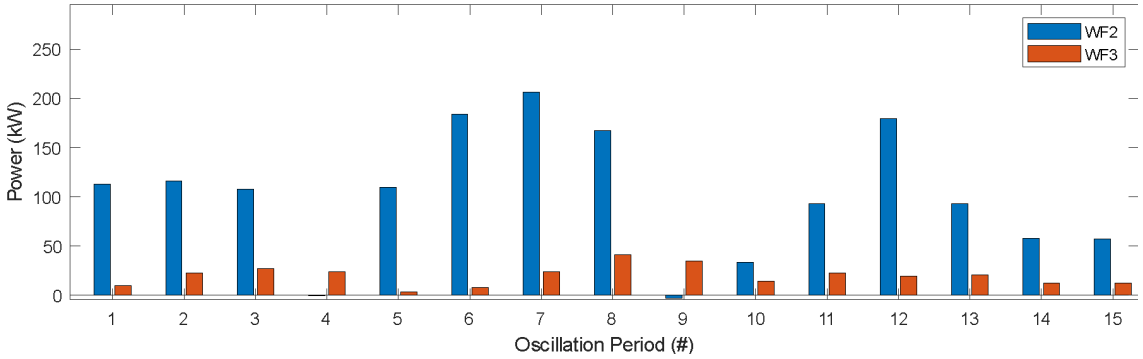


Figure 27. 63.5 Hz interharmonic power out of windfarms WF2 and WF3.

5.1.2.2 Case of a Solar Farm

The second example is about a 10-MW solar farm connected to a 44-kV feeder. The energization of a shunt capacitor nearby triggered oscillation of the solar farm's current as shown in Figure 28. A beating pattern can be clearly seen in the current waveforms. The beating frequency is about 23 Hz. The current spectrum and interharmonic powers are shown in Figure 29. Since the oscillation period is short, the entire available data is used to extract interharmonics in order to get higher interharmonic frequency resolution. (The frequency resolution, defined as the number of spectral bins between two harmonic frequencies, is proportional to the length of the data window). The results show that there is one large interharmonic around 84 Hz. The 84 Hz interharmonic power enters the grid, implying the solar farm is a source of oscillation. Inverter PLL malfunction resulting from 84 Hz capacitor-caused parallel resonance was suspected as the cause (Li, 2018).

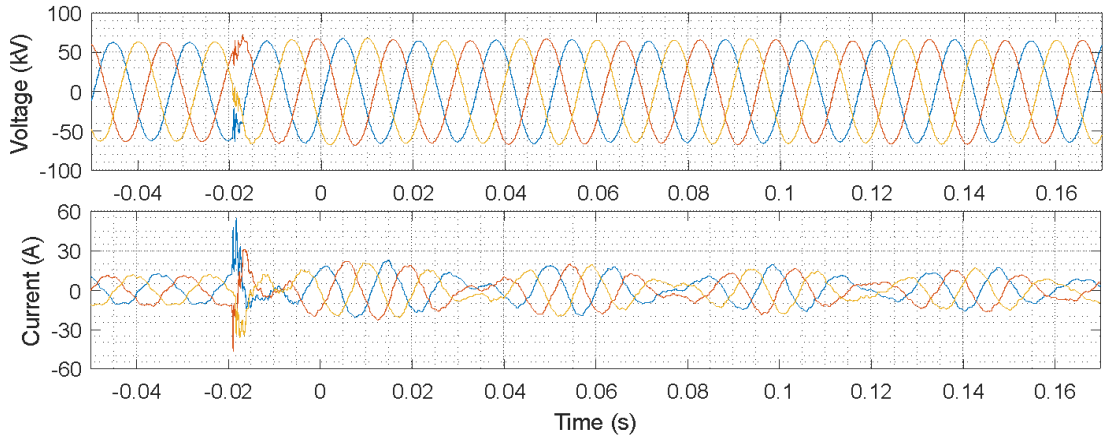


Figure 28. Three-phase voltage and current waveforms of a solar farm.

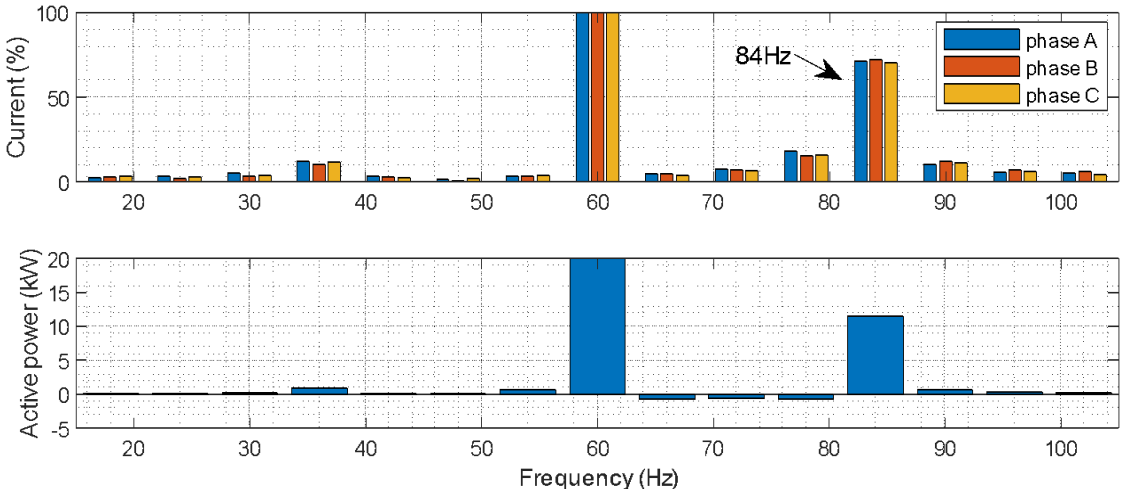


Figure 29. Spectrums of current and interharmonic power of the solar farm.

It is important to note that the interharmonic frequency of 84 Hz is quite different from that of the fundamental frequency. As a result, the impedances in a power system can be quite different at 84 Hz versus 60 Hz. This phenomenon raises an important question: it may not be reliable to use 60 Hz impedances and phasors for IBR oscillation assessment. This observation is also supported by (Fan L. , et al., 2022) which shows three subsynchronous oscillation cases that involve interharmonic components of frequencies far different from 60 Hz.

5.2 Modeling and Prediction of IBR Dynamic Response

Waveform and synchro-waveform measurements can also be used to model and predict the dynamic response of IBRs. This can be done through both statistical methods (Ahmadi-Gorjayi & Mohsenian-Rad, 2023) and machine learning methods (Yazdi, Ahmadi-Gorjayi, & Mohsenian-Rad, 2025). The process is shown in Figure 30.

Figure 30(a) shows the raw real-world waveform measurements that are recorded by a WMU at an IBR during a system-wide disturbance in the power system. Only one phase is shown here. The voltage waveform measurements are denoted by $v(t)$ and the current waveform measurements are denoted by $i(t)$. A disturbance in the power system causes a momentary voltage oscillation event at the location of the PV inverter that lasts only about half of an AC

cycle. The change in voltage in turn causes a dynamic response in the IBR's current waveforms, which is transient and oscillatory. Such waveform measurements can be used to model this dynamic response at the waveform level, relying solely on data-driven methods based on the waveform measurements at the IBR, without requiring access to the internal physical models of the IBR components.

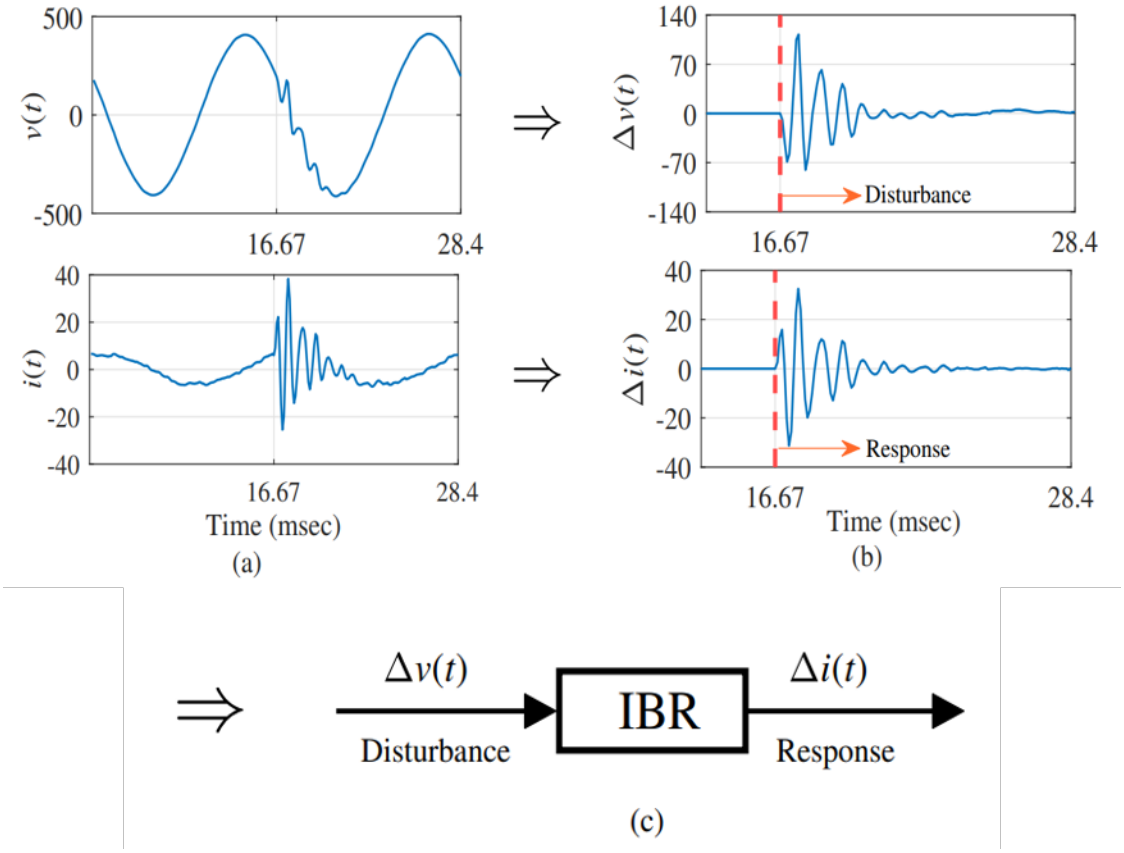


Figure 30. The process to model the dynamic response of IBRs to sub-cycle disturbances using waveform measurements: (a) a sub-cycle voltage oscillation event in the power system, which in turn causes agitation in the injected current by the IBR; (b) the corresponding differential waveforms that capture the signatures of the sub-cycle disturbance and the signatures of the sub-cycle response of the IBR; (c) a data-driven model for the input-output relationship between the sub-cycle disturbance and the sub-cycle response of the IBR.

Figure 30(b) shows the differential waveforms corresponding to the raw voltage and current measurements from Figure 30(a). Given a waveform measurement $x(t)$, its corresponding differential waveform $\Delta x(t)$ is defined as the difference between $x(t)$ and a delayed version of $x(t)$. Mathematically, the differential waveform can be expressed as follows [from (Mohsenian-Rad H. , 2022) Section 4.2.5]:

$$\Delta x(t) = x(t) - x(t - T),$$

where t is the start of the event and $T = 1/60$ seconds is the waveform interval. Compared with the raw waveforms in Figure 30(a), the differential waveforms in Figure 30(b) provide a clearer signature of the sub-cycle disturbance and a clearer signature of the response of the IBR.

Finally, Figure 30(c) shows the input-output (black-box) relationship between $\Delta v(t)$ and $\Delta i(t)$, i.e., the differential waveform signatures of the sub-cycle disturbance that is obtained from $(v(t)$, and the differential waveform signatures of the response of the IBR that is obtained from $i(t)$.

The details of the methodologies to obtain such an input-output model are discussed in (Ahmadi-Gorjayi & Mohsenian-Rad, 2023) and (Yazdi, Ahmadi-Gorjayi, & Mohsenian-Rad, 2025), including the use of statistical and machine learning methods. The resulting models can be used for condition monitoring and diagnostics at IBRs. Apart from comparing the behavior of similar IBRs to identify abnormal dynamics, the models can also detect any significant changes in the dynamic behavior of each IBR, indicating potential failures that may require site inspection.

The data-driven methods can also help develop digital twins for IBRs, to predict their responses to various power system disturbances and to prevent undesirable tripping. Digital twins are being increasingly used in power networks and other cyber–physical systems for diverse applications; see (Tao, Zhang, Liu, & Nee, 2019). The analysis in this section can also be employed to compare the dynamic responses of IBRs in a region to predict ripple effects, such as momentary IBR disruption, that may follow certain system-wide disturbances.

5.3 Generator Scorecard

The Generator Scorecard tool, developed by Pacific Northwest National Laboratory and Bonneville Power Administration (BPA), enables a user to go through live or archived PMU data and observe the response of individual power plants or the system as a whole to voltage and frequency excursion events (Follum, Mana, Mitchell-Colgan, & Faris, 2025). The tool also monitors deviations of power plants from scheduled voltage settings. In addition, a graphical user interface (GUI) developed for the Generator Scorecard enables users to go through a large amount of event and power plant response data, group the information, discard unsuitable events, and analyze individual power plants easily while also seamlessly switching between individual plant performance and the whole balancing authority performance (Follum, et al., 2024). The tool provides a platform to monitor IBR responses to events in the grid and can be extended to set up specific requirements based on the expected performance from different kinds of IBRs based on their types and interconnection requirements. An initial study was done in collaboration with BPA by installing the software in BPA's synchrophasor lab. A commercial version of the tool is available at (Simple Thread, 2026).

In the initial set of studies, three performance aspects are considered. The first analytic for frequency response measure (FRM) automatically identifies deviations in system frequency from the nominal 60 Hz and evaluates how much a power plant responds by adjusting its output of active power. The voltage response measure (VRM) portion of the Generator Scorecard is very similar to the frequency response portion except that plant responses in reactive power are considered following shifts in voltage magnitude. The final analysis in the Generator Scorecard monitors the percentage of each minute that the power plant's voltage falls outside of its assigned voltage schedule.

5.3.1 Frequency Response Measure (FRM)

The frequency response measure is defined to quantify a single plant's contribution to stabilizing system frequency following a disturbance, using only local measurements of frequency and active power. The methodology consists of an automated frequency excursion detector, an estimator for the excursion start time, and a calculation formula that mirrors the balancing

authority-level FRM but applied at the plant level. The input to the detector is a sequence of frequency measurements from a phasor measurement unit, with the nominal 60 Hz component removed by subtracting the first sample from all subsequent samples. This preprocessing step centers the signal around zero and prepares it for low-pass filtering to emphasize the large-scale trends associated with system-wide frequency excursions, rather than high-frequency noise or local oscillations.

Once a frequency excursion is detected, the next step is to identify the excursion start time and key points in the frequency trajectory that will be used in the FRM calculation. These points are labelled *A*, *B*, and *C* in Figure 31 and represent characteristic features of the excursion, such as the pre-disturbance baseline, the nadir or peak of the excursion, and an intermediate point defining the interval of interest. For an under-frequency event, for example, A_F denotes the frequency at the pre-event baseline, B_F the frequency after the system has responded, and *C* an earlier point used for screening.

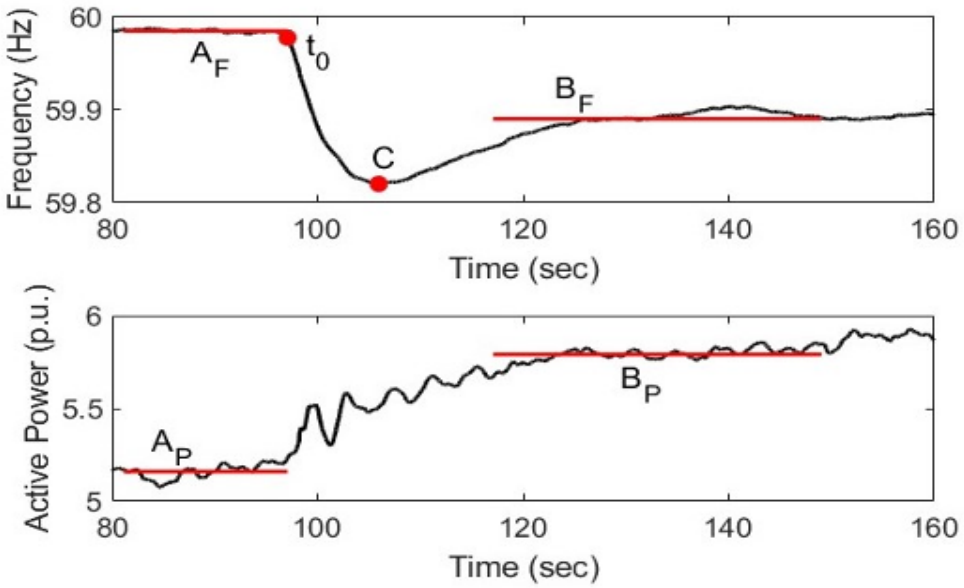


Figure 31. Illustration of the inputs to the FRM calculation for Signature 2463 under Provider 10 in the Grid Event Signature Library (ORNL, LLNL, PNNL, 2024).

Events are filtered to ensure they exhibit the characteristic shapes associated with true excursions rather than transient oscillations. Only events for which the maximum frequency between the indices corresponding to C and a fixed time after the estimated start, $(t_0 + 20)$ seconds, remains below the baseline A_F are retained for under-frequency events. This is expressed as

$$\left(F\left(k_C, k_C + 1, \ldots, k_{t_0+20}\right)\right) < A_F$$

which eliminates cases where frequency briefly overshoots the baseline and behaves more like an oscillation than a sustained excursion. Additional shape checks require that under-frequency excursions satisfy $A_F > B_F$ and over-frequency excursions satisfy $A_F < B_F$, ensuring that the identified events have the expected monotonic deviation and partial recovery behavior. Only events passing these checks proceed to FRM calculation.

For each accepted event, the FRM is calculated from measurements of active power and frequency associated with the plant. Let A_P and B_P denote the plant's active power output at the pre-event and post-response conditions corresponding to A_F and B_F. The plant-level FRM is then defined as

$$FRM = \frac{B_P - A_P}{10\,(B_F - A_F)}$$

with units of MW per 0.1 Hz. This formula parallels the balancing authority FRM, but applied to an individual plant rather than an entire area. For under-frequency events, the numerator $(B_P - A_P)$ is negative if the plant increases active power output in response to the frequency drop, which is the desired behavior; for over-frequency events, where frequency rises above nominal, the numerator is positive when the plant decreases active power, again contributing to restoration of frequency. Larger negative values of FRM indicate that the plant is making a larger contribution, per unit of frequency deviation, to returning the frequency toward nominal. Positive FRM values indicate counter-productive behavior, where the plant's active power changes in a way that exacerbates the frequency deviation. By automating the detection of excursions, the identification of key points, and the computation of FRM, the method enables systematic evaluation of plant frequency response across many events without the need for manual selection and analysis of individual disturbances.

Figure 32 provides power plant performance through all the events during the period of observance. Each point in the plot represents the response of a plant to a frequency excursion. As desired, Plant 2 consistently increased MW output following drops in frequency (lower-right quadrant) and decreased MW output following rises in frequency (upper-left quadrant). As a result, it had consistently large and negative FRM values. In contrast, Plant 1 did not respond to frequency excursions, so its reported change in MW output is small and essentially random.

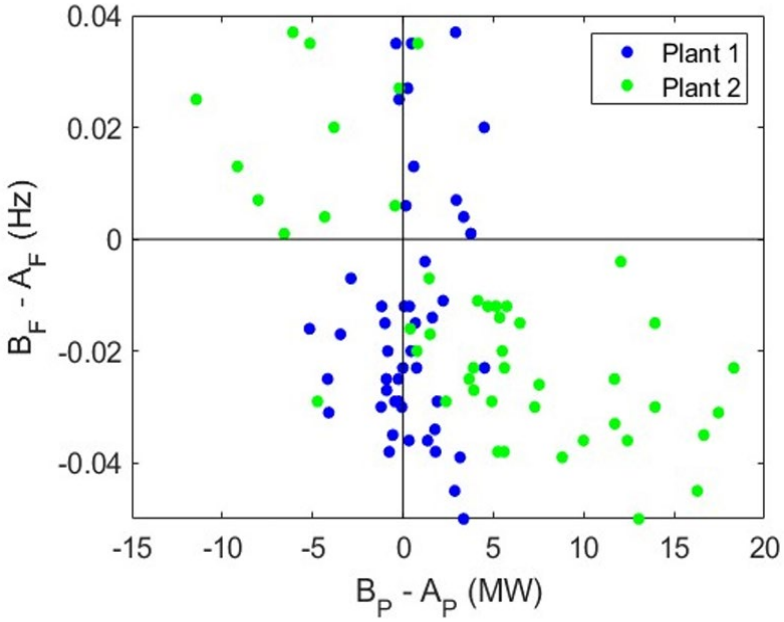


Figure 32. Summary of responses from two power plants for all frequency excursions analyzed during the field demonstration. Plant 1 shows inconsistent performance, while Plant 2 regularly adjusts active power up for under-frequency excursions and down for over-frequency excursions.

5.3.2 Voltage Response Measure (VRM)

The voltage response measure is designed to quantify a plant's adjustment of reactive power following a sudden change in the voltage magnitude at its POI, thereby indicating whether the plant supports voltage stability by providing appropriate reactive power support. The VRM methodology comprises two main components: a voltage excursion detector, which identifies periods when the local voltage is persistently outside a normal band, and a calculation procedure that relates changes in reactive power to changes in voltage using a set of reference points on the measured trajectories.

The voltage excursion detector operates on a sequence of voltage magnitude measurements $V(k)$ and is based on the idea that a significant excursion occurs when voltage remains outside predefined lower and upper thresholds for a sufficient length of time. Let γ_V^- and γ_V^+ denote the lower and upper voltage thresholds, respectively. An indicator function $I(k)$ is defined over the most recent K samples as

$$I(k) = \begin{cases} 0, \gamma_V^- \le V(k) \le \gamma_V^+ \\ 1, otherwise \end{cases}$$

so that $I(k)$ flags samples where the voltage lies outside the thresholds. A voltage excursion is detected when the sum of this indicator over the most recent K samples exceeds or equals a parameter γ_I,

$$\sum_{k=1}^{K} I(k) \ge \gamma_I,$$

meaning that voltage has been outside the acceptable range for at least γ_I of the last K samples. For the results presented, γ_I and K were set to values equivalent to 30 and 35 seconds, respectively, ensuring that only sustained excursions, rather than brief spikes, trigger analysis. The thresholds γ_V^- and γ_V^+ are not fixed but are continuously updated by applying negative and positive deviations to a baseline voltage. This baseline is established by averaging the most recent window of measurements—180 seconds in the reported results—so that the thresholds track slow changes in nominal voltage level. The magnitude of the deviations used to define the thresholds is location-dependent and selected based on measurement review. For example, in one set of results, the chosen deviations across buses ranged from 0.5 to 2.1 kV line-to-line, reflecting differing nominal voltages and system stiffness at each location.

Once a voltage excursion has been detected at the POI, VRM is computed from the joint behavior of the local voltage and the plant's reactive power output. Figure 33 illustrates this methodology using a simulation of a wind power plant's response to capacitor switching, in which real field measurements of frequency and voltage at the point of interconnection are played into a collector system model with an aggregate generator. In this example, baseline quantities A_V and A_Q are defined as the averages of voltage and reactive power over the five seconds preceding the event capturing pre-disturbance operating conditions. The points C_V and C_Q mark the beginning of the plant's reactive power response and are chosen as the voltage and reactive power at the first sample after the voltage magnitude has rebounded from its most extreme value following the switching action. Settling values B_V and B_Q are then defined as the averages of voltage and reactive power over a window from two to four seconds after C_V and C_Q representing the post-response steady condition. With these six quantities defined, the plant's

reactive power response is quantified as $(B_Q - C_Q)$, and the associated change in voltage is $(B_V - C_V)$.

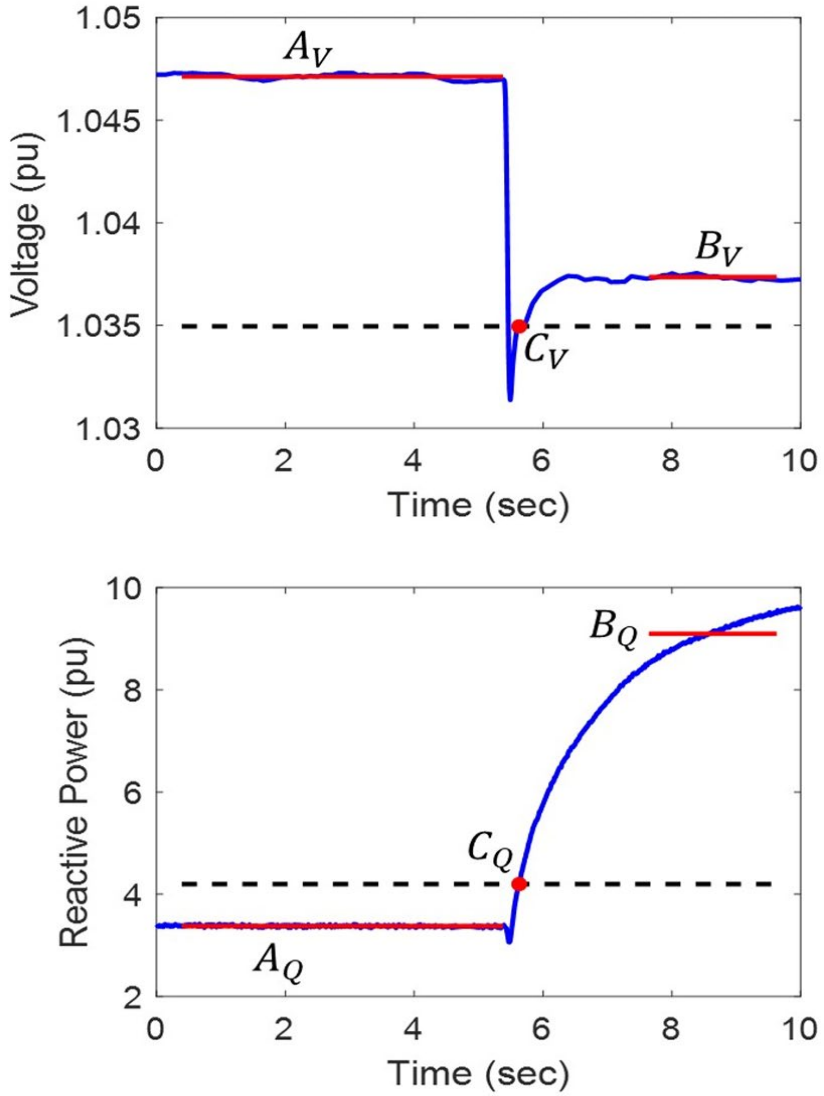


Figure 33. Simulation of a wind power plant's appropriate response in reactive power (bottom) to a sudden change in voltage at the point of interconnection (top).

The VRM is constructed to be large when the plant provides a strong, appropriately directed reactive power response to support voltage recovery and the VRM is designed to be relatively insensitive to absolute voltage level and system stiffness. It is defined as

$$VRM = \frac{B_Q - C_Q}{|C_Q - A_Q|} \times \frac{B_V - C_V}{|C_V - A_V|}$$

The numerator of the first factor captures the plant's incremental reactive power contribution during the recovery phase, while the numerator of the second factor captures the incremental change in voltage over the same period. The denominators scale these changes by the magnitudes of the initial reactive power and voltage deviations between baseline and the start of

response, $|C_Q - A_Q|$ and $|C_V - A_V|$, respectively. This scaling normalizes the metric across locations with different nominal voltages and levels of system stiffness and cancels units so that VRM is dimensionless. Large positive values of VRM are desirable – they indicate that reactive power increased in response to a voltage drop or decreased in response to a voltage rise, in a way that supports movement of voltage back toward its baseline.

In the reference simulation of appropriate plant behavior, the VRM was 1.17, reflecting a strong voltage support response. To demonstrate the metric's ability to identify under-performing plants in simulation, the plant's controller parameters were then modified to represent a plant that is not operating in voltage-control mode, a situation that does occur in practice. When the simulation was repeated with the same voltage and frequency inputs, the reactive power response was much weaker, and the VRM dropped to 0.07, clearly signaling poor voltage support performance. This example shows how VRM translates the qualitative notion of "good" or "bad" reactive power behavior into a quantitative, comparable metric that can be used within the Generator Scorecard to flag plants whose voltage control performance requires further investigation.

The response of all the plants from measurement data during field demonstration is shown in Figure 34. Each point in the plot represents a power plant's response to one of the studied events. Points in the first and third quadrants demonstrate a desirable response of the power plants by absorbing or providing reactive power to increase or drop the voltage accordingly. Thus, the results indicate that the system as a whole is responding appropriately to voltage excursions.

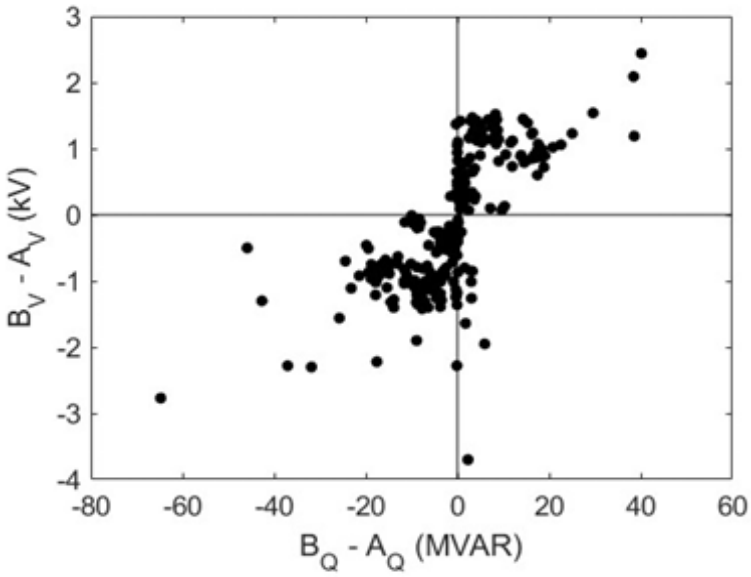


Figure 34. Summary of all voltage excursions analyzed during the field demonstration. Clustering in quadrants 1 and 3 indicate that plants across the territory appropriately adjusted reactive power.

The results of the field demonstration at BPA validated the ability of the application to summarize the frequency and voltage control performance of power plants. These measurement-based summaries are useful in identifying plants for further review with model-based approaches.

6.0 Conclusion

This report examined the motivation, considerations, and methods for monitoring IBRs and analyzing their performance in a grid that is increasingly changing due to the integration of power electronics-based generation and loads. The behaviors most relevant to IBR performance often occur on time scales and in forms that SCADA cannot capture. As a result, effective monitoring depends not on a single tool or data stream, but on selecting and combining measurement technologies that match the speed, fidelity, and context required to understand how IBRs behave during both normal operation and disturbances.

The report discussed several real-world use cases that demonstrate the value of high-resolution monitoring for IBRs. These include analysis of emerging dynamic behaviors, oscillation detection, oscillation source localization, monitoring, diagnostics, and fault response analysis. The real-world experiences reinforce that correct measurement placement and synchronized comparison are essential to interpreting IBR behavior correctly.

The report also discussed advanced analytics to further expand the capabilities of these measurements. These include the use of interharmonics to understand the oscillatory behavior of IBRs, advanced modeling and prediction of IBR dynamic responses, and the use of measurements to automatically evaluate the response of generators to system events.

The report connects these monitoring approaches to evolving standards and requirements intended to address known data gaps. It briefly discussed NERC recommendations and relevant IEEE standards, and similar monitoring expectations in Europe through the EU Network Code on Requirements for Generators, which requires real-time or near-real-time communication and telemetry for relevant generators.

To conclude, the report advocates a hybrid monitoring approach of leveraging both PMU and POW technologies and aligning them with status, event, and supervisory context as the most effective path toward ensuring reliability, stability, and efficient operation as power systems continue to transition to higher penetrations of IBRs. Some promising directions for future whitepapers from technical working groups would include discussions on implementation guidelines, incorporation of large loads, and use of Artificial Intelligence (AI) in performance measurement analytics.

7.0 References

Agrawal, U., Bohlen, J., Hiebert, J., & Penne, K. (2024). Real-time monitoring and mitigation and offline analysis of forced oscillations in RC West (CAISO). *Hawaii International Conference on System Sciences (HICSS).* Waikiki, HI.

Ahmadi-Gorjayi, F., & Mohsenian-Rad, H. (2022). Physics-Aware Sparse Harmonic State Estimation in Power Distribution Systems. *IEEE PES Innovative Smart Grid Technologies Conference.* Washington, DC.

Ahmadi-Gorjayi, F., & Mohsenian-Rad, H. (2023). Data-Driven Models for Sub-Cycle Dynamic Response of Inverter-Based Resources Using WMU Measurements. *IEEE Transactions on Smart Grid*, vol. 14, no. 5, pp. 4125-4128.

Becejac, T., Follum, J., Vartanian, C., & Cain, N. (2020). *Identification and Evaluation of Oscillations in the Cordova, Alaska Microgrid.* Retrieved from https://www.naspi.org/sites/default/files/2026-06/03_pnnl_follum_cordova_alaska_20201105.pdf

Biswas, S., & Follum, J. (2025). *Interpreting Forced Oscillation Notifications from ESAMS: General Guidance for Reliability Coordinators.* Richland: Pacific Northwest National Laboratory.

Biswas, S., Chatterjee, K., Follum, J. D., & Kincic, S. (2024). *Offline Power Systems Applications Enabled by Phasor Measurement Units: Technical Assistance to the Power Sectors of Southeast Asia.* https://doi.org/10.2172/2479751.

Biswas, S., Follum, J., Ramesh, M., Chatterjee, K., Mana, P., & Doty, J. (2026). Oscillation Detection, Characterization, and Source Localization Using Point-on-Wave Measurements. *International Conference on Smart Grid Synchronized Measurements and Analytics.* Santiago de Chile.

Biswas, S., Tuffner, F., Follum, J., & Wall, T. (2024). Inverter Model Validation and Calibration Using Phasor Measurement Unit Data. *IEEE Access*, vol. 12, pp. 98990-99001.

Chatterjee, K., Biswas, S., Follum, J., & Kincic, S. (2023). *Online Monitoring Applications Enabled by Phasor Measurement Units: Technical Assistance to the Power Sectors of Southeast Asia.* Pacific Northwest National Laboratory.

Chatterjee, K., Follum, J., Varghese, A., Biswas, S., Farantatos, E., & Zhu, L. (2026). *Measurement Adequacy for Monitoring Data Center Oscillations.* Retrieved from https://www.naspi.org/documents/measurement-adequacy-monitoring-data-center-oscillations

Chen, Y., & Nayak, N. (2023). *PJM Use Case of SynchrophasorsAutomated Generator Model Validation (AGMV).* Retrieved from NASPI Working Group meeting: https://www.naspi.org/events/naspi-work-group-hybrid-meeting-and-vendor-show-1

Cooke, T. (2025, October). *Flicker Detection with Optimized Continuous Point-OnWave (CPOW) Monitoring and Data Visualization.* Retrieved from Point on Wave Application conference: https://powaconference.org/presentations/session_1/Flicker%20Detection%20with%20Optimized%20Continuous%20Point-On-Wave%20(CPOW)%20Monitoring%20and%20Data%20Visualization.pdf

Dong, S., Wang, B., Tan, J., Kruse, C. J., Rockwell, B. W., & Hoke, A. (2023). *Analysis of November 21, 2021, Kauai Island power system 18-20 Hz oscillations.* arXiv preprint arXiv:2301.05781.

Ehsani, N., Ahmadi-Gorjayi, F., Ye, Z., McEachern, A., & Mohsenian-Rad, H. (2023). Sub-cycle Event Detection and Characterization in Continuous Streaming of Synchro-waveforms: An Experiment Based on GridSweep Measurements. *IEEE North American Power Symposium.* Asheville, NC.

ENTSO-E. (2016). *Real Time Data and Communication: ENTSO-E Guidance Document for National Implementation for Network Codes on Grid Connection.* Retrieved from https://eepublicdownloads.entsoe.eu/clean-documents/Network%20codes%20documents/NC%20RfG/161116_IGD_RealTimeDataMonitoring_for%20publication.pdf

ENTSO-E. (2026). *Requirements for Generators.* Retrieved from https://www.entsoe.eu/network_codes/rfg/

Etingov, P., S, B., Follum, J, Y. T., Ahmad, T., Chatterjee, K., & Varghese, A. (2025). Evaluating a Generic DER Aggregation Dynamic Model Using Open-Access Phasor Measurements. *IEEE PES General Meeting.*

Fan, L., Miao, Z., S., S., K. P., Gevorgian, V., & Fu, J. (2022). *Data-driven dynamic modeling in power systems: A fresh look on inverter-based resource modeling.* IEEE Power and Energy Magazine, 20(3), 64-76.

Fan, L., Miao, Z., Shah, S., Cheng, Y., Rose, J., Huang, S., . . . Zhu, S. (2022). Real-world 20-Hz IBR subsynchronous oscillations: Signatures and mechanism analysis. *EEE Transactions on Energy Conversion*, 37(4), pp.2863-2873.

Follum, J. D., Agalgaonkar, Y., Hovsapian, R., Lacommare H., K., MacDonald, J., McEachern, A., . . . Mana, P. (2024). *PROGRESS MATRIX Final Report.* Pacific Northwest National Laboratory.

Follum, J., Mana, P., Mitchell-Colgan, E., & Faris, A. (2025). Automated Evaluation of Power Plant Frequency and Voltage Control using Synchrophasors. *58th Hawaii International Conference on System Sciences.* Big Island, HI.

Halliday, C. (2018). *Visualisation of Real Time System Dynamics using Enhanced Monitoring (VISOR).*

IEEE Std 1453-2015. (2015). *IEEE recommended practice for the analysis of fluctuating installations on power systems.*

IEEE Std C37.118.1-2011. (2011). *IEEE standard for synchrophasor measurements for power systems.*

IEEE Std. 2800-2022. (2022). *Interconnection and Interoperability of Inverter-Based Resources (IBRs) Interconnecting with Associated Transmission Electric Power Systems.*

Kosterev, D., Burns, J., Leitschuh, N., Anasis, J., Donahoo, A., Trudnowski, D., . . . Pierre, J. (2016). Implementation and Operating Experience with Oscillation Detection Application at Bonneville Power Administration. *CIGRE US National Committee, 2016 Grid of the Future Symposium.*

Lackner, C., & Carroll, R. (2025). *Distributed Waveform Analytics in the WaveApps Platform.* Retrieved from Point on Wave Applications Conference: https://powaconference.org/presentations/session_5/Distributed%20Waveform%20Analytics%20in%20the%20Wave%20Apps%20Platform.pdf

Li, C. (2018). Unstable operation of photovoltaic inverter from field experiences. *IEEE Transactions on Power Delivery*, vol. 33, no.2, pp. 1013-1015.

Li, C., & Reinmuller, R. (2019). Asset condition anomaly detections by using power quality data analytics. *IEEE PES General Meeting.* Atlanta, GA, USA.

Luo, X. (2023). *IBR Model Verification Using Measurement Playback Method.* Retrieved from NASPI working group meeting: https://www.naspi.org/events/naspi-work-group-hybrid-meeting-and-vendor-show-1

Maslennikov, S. (2024). Enhancing the Efficiency of Locating the Oscillation Source. *IEEE Transactions on Power Systems*.

Maslennikov, S., Wang, B., & Litvinov, E. (2017). Dissipating Energy Flow Method for Locating the Source of Sustained Oscillations. *International Journal of Electrical Power & Energy Systems.* .

Mishra, C., Vanfretti, L., Delaree, J., & Jones, K. D. (2024). Analyzing a Non-Sinusoidal Response from a Real-World Solar PV. *IEEE Transactions on Power Systems*, 39(2), 4771-4774.

Mohsenian-Rad, H. (2022). *Smart Grid Sensors: Principles and Applications.* Cambridge University Press, Cambridge, U.K.

Mohsenian-Rad, H., & Kezunovic, M. a. (2025). *Synchro-Waveforms in Wide-Area Monitoring, Control, and Protection: Real-World Examples and Future Opportunities.* IEEE Power and Energy Magazine, vol. 23, no. 1, pp. 69-80.

Mohsenian-Rad, H., & Khaledian, P. (2022). Automated Event Region Identification and its Data-Driven Applications in Behind-the-Meter Solar Farms Based on Micro-PMU Measurements. *IEEE Transactions on Smart Grid*, 2094-2106.

Mohsenian-Rad, H., Joo, J., Balestrieri, M., Piyasinghe, L., Biswas, S., Chatterjee, K., . . . L. Chen, J. F. (2024). *Synchro-waveform measurements and data analytics in power systems.* EEE Power & Energy Society Technical Report.

Mueller, D. (2007). Case Studies of Harmonic Problems, Analysis, & Solutions on Transmission Systems. *9th International Conference on Electrical Power Quality and Utilisation.* doi:https://doi.org/10.1109/EPQU.2007.4424179

Mulawarman, A., & Mysore, P. (2011). Detection of undamped subsynchronous oscillations of wind generators with series compensated lines. *Minnesota Power Systems Conference.*

NERC. (2017). *1200 MW Fault Induced Solar Photovoltaic Resource Interruption DIsturbance Report.* Retrieved from https://www.nerc.com/our-work/reports/event-analysis-reports

NERC. (2018). *900 MW Fault Induced Solar Photovoltaic Resource Interruption Disturbance Report.* Retrieved from https://www.nerc.com/our-work/reports/event-analysis-reports

NERC. (2021). *Odessa Disturbance.* Retrieved from https://www.nerc.com/our-work/reports/event-analysis-reports

NERC. (2022). *2022 Odessa Disturbance.* Retrieved from https://www.nerc.com/our-work/reports/event-analysis-reports

NERC. (2025). *PRC-028-1 – Disturbance Monitoring and Reporting Requirements for Inverter-Based Resources.* Retrieved from https://www.nerc.com/standards/reliability-standards/prc/prc-028-1

NERC. (2026). NERC PRC-029-2 - Frequency and Voltage Ride-through Requirements for Inverter-Based Resources Reliability Standard. Retrieved from https://www.nerc.com/standards/reliability-standards/prc/prc-029-2

NERC Alert Level III. (2025, May 20). *Essential Actions to Industry - Inverter-Based Resource Performance and Modeling .* Retrieved from NERC: chrome-extension://efaidnbmnnnibpcajpcglclefindmkaj/https://www.nerc.com/globalassets/programs/bpsa/alerts/2023/level-3-alert-essential-actions-ibr-performance-and-modeling.pdf

ORNL, LLNL, PNNL. (2024, May 23). *Grid Event Signature Library*. Retrieved from https://gesl.ornl.gov

Pudasaini, B., Vanfretti, L., Mishra, C., De La Ree, J., & Jones, K. D. (2025). Dynamic Performance Analysis of an Inverter-Based PV Plant during Sunrises and Sunsets through Synchrophasors. *IEEE Power & Energy Society General Meeting (PESGM).*

Purcell, T. J., Wold, J., Khan, M. A., & Bestebreur, J. (2025). Case Study: Enhancing Grid Reliability in the Presence of Inverter-Based Resources Through Advanced Oscillation Detection and Mitigation. *Annual Western Protective Relay Conference.* Spokane, WA.

Rhodes, M., & and Goodrich, D. (2024). *Recent BESS Oscillations: Root Cause Analysis and Wide-Area Impacts.* NASPI Webinar.

Silverstein, A., Kosterev, D., Yang, S., & VanZandt, V. (2014). Model Validation Using SYnchrophasor Data -- A Synchrophasor Success Story. *CIGRE US National Committee, 2014 Grid of the Future Symposium.*

Simple Thread. (2026, May 1). *AION Pulse*. Retrieved from simplethread.com: https://www.simplethread.com/solutions/aion-pulse/

Tao, F., Zhang, H., Liu, A., & Nee, A. Y. (2019). Digital twin in industry: State-of-the-art. *IEEE Transactions on Industrial Informatics*, vol. 15, no. 4, pp. 2405–2415.

Tayjasanant, T., & Xu, W. (2004). A case study of flicker/interharmonic problems caused by a variable frequency drive. *Proc. ICHQP.* Lake Placid, NY.

Tong, L., Wang, X., & Zhao, Q. (2025). Grid Monitoring with Synchro-Waveform and AI Foundation Model Technologies. *IEEE Transactions on Smart Grid*.

von Meier, A., & Enas, A. (2025, April 15). *Active and Localized measurement of Grid Inertia.* Retrieved from NASPI Working Group meeting Spring 2023: https://www.naspi.org/sites/default/files/2026-06/01_03_02_VonMeier_ReactiveTechnologies_20250415.pdf

Wang, C., Mishra, C., Jones, K. D., Gardner, R. M., & Vanfrett, L. (2022). Identifying Oscillations Injected by Inverter-Based Solar Energy Sources. *IEEE Power & Energy Society General Meeting (PESGM).* Denver, CO, USA.

Xie, X., Zhan, Y., Shair, J., Ka, Z., & Chang, X. (2019). Identifying the source of subsynchronous control interaction via wide-area monitoring of sub/super-synchronous power flows. *IEEE Transactions on Power Delivery*, 2177-2185.

Xu, W., Huang, Z., Xie, X., & Li, C. (2022). Synchronized Waveforms – A Frontier of Data-Based Power System and Apparatus Monitoring, Protection, and Control. *IEEE Trans. on Power Delivery*.

Xu, W., Yong, J., Marquez, H., & Li, C. (2025). Interharmonic Power – A New Concept for Power System Oscillation Source Location. *IEEE Transactions on Power Systems*.

Yazdi, H. M., Li, C., & Mohsenian-Rad, H. (2025). IBR Responses during a Real-World System-Wide Disturbance: Synchro-Waveform Data Analysis, Pattern Classification, and Engineering Implications. *IEEE Transactions on Smart Grid*, vol. 16, no. 4, pp. 3453-3456. .

Yazdi, H., Ahmadi-Gorjayi, F., & Mohsenian-Rad, H. (2025). Data-Driven Modeling of Sub-Cycle Dynamics of Inverter-based Resources Using Real-World Synchro-Waveform Measurements. *IEEE Transactions on Power Delivery*.

Yin, H., Qiu, W., Wu, Y., W., Y., Tan, J., & Hoke, A. (2025). Anomaly Identification of Synchronized Voltage Waveform for Situational Awareness of Low Inertia Systems. *IEEE Trans. on Smart Grid*, vol. 16, no. 3, pp. 2416-2428.

Yunzhi, C., Lingling, F., Jonathan, R., Shun-Hsien, H., John, S., Xiaoyu, W., . . . al., e. (2022). Real-world subsynchronous oscillation events in power grids with high penetrations of inverter-based resources. *IEEE Transactions on Power Systems*, 316-330.



Pacific Northwest National Laboratory

902 Battelle Boulevard
P.O. Box 999
Richland, WA 99354

1-888-375-PNNL (7665)

www.pnnl.gov